JACS Au
AN OPEN ACCESS JOURNAL OF THE AMERICAN CHEMICAL SOCIETY

pubs.acs.org/jacsau
Perspective

Nanopore Environmental Analysis

Xiaofeng Lu,[▽] Xiaoyu Du,[▽] Dong Zhong, Renjie Li, Junjie Cao, Shuo Huang,* and Yuqin Wang*

Cite This: JACS Au 2025, 5, 1570−1590

ABSTRACT: As global pollution continues to escalate, timely and accurate monitoring is essential for guiding pollution governance and safeguarding public health. The increasing diversity of pollutants across environmental matrices poses a significant challenge for instrumental analysis methods, which often require labor-intensive and time-consuming sample pretreatment. Nanopore technology, an emerging single-molecule technique, presents a promising solution by enabling the rapid identification of multiple targets within complex mixtures with minimal sample preparation. A wide range of pollutants have been characterized using natural biological nanopores or artificial solid-state nanopores, and their distinct advantages include simple sample preparation, high sensitivity, and rapid onsite analysis. In particular, long-read nanopore sequencing has led to dramatic improvements in the analyses of environmental microbial communities, allows species-level taxonomic assignment using amplicon sequencing, and simplifies the assembly of metagenomes. In this Perspective, we review the latest advancements in analyzing chemical and biological pollutants through nanopore sensing and sequencing techniques. We also explore the challenges that remain in this rapidly evolving field and provide an outlook on the potential for nanopore environmental analysis to transform pollution monitoring, risk assessment, and public health protection.

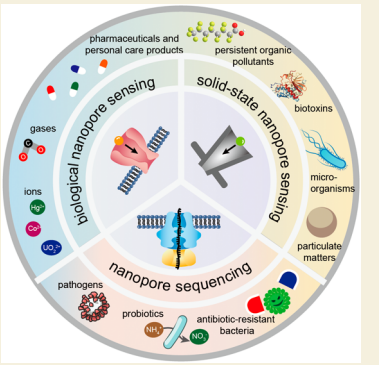

KEYWORDS: *nanopore sensing, nanopore sequencing, chemical pollutants, biological pollutants, environmental analysis*

1. INTRODUCTION

The rapid industrialization and urbanization of recent decades have led to the release of a wide range of pollutants into the environment, including traditional contaminants such as heavy metals and pesticides, as well as emerging threats such as pharmaceuticals, pathogens, microplastics, and nanomaterials.[1] The increasing diversity and complexity of these pollutants have significantly increased the challenges of environmental monitoring. Many pollutants belong to large families with similar structures, such as short-chain chlorinated paraffins, which consist of more than 7,000 congener types.[2] These pollutants are often present at trace levels, typically in the milligram (mg/L) to microgram (μg/L) per liter range, with certain persistent organic pollutants (POPs) and pharmaceutical and personal care products (PPCPs) detected at nanogram (ng/L) concentrations. The structural similarities within these families, combined with their low concentrations, complicates the separation, enrichment, and discrimination of the target analytes. Moreover, the compositions and abundances of pollutants fluctuate over time and space and are influenced by factors such as weather and hydrological conditions. These dynamic variations require monitoring techniques that are capable of fast, onsite, and real-time analyses for accurate, timely assessments of environmental pollution. While advanced instrumental techniques, such as atomic spectroscopy,[3] molecular spectroscopy,[4] chromatography,[5] and mass spectrometry,[6] are highly effective, they often involve labor-intensive sample preparation and require large and precise instruments, which are not always suited to meet current demands.

Over the past few decades, nanopore technology has gradually been adopted for the detection of environmental pollutants and demonstrates distinct advantages over traditional methods.[7−9] A nanopore sensor is typically defined as a nanoscale aperture in an impermeable membrane, spanning two electrolyte-filled reservoirs. When a voltage is applied, the translocation of analytes through the nanopore generates characteristic ionic current modulations, enabling molecular identification. This ability to analyze individual molecules in complex environmental matrices allows direct analysis without the need for extensive sample preparation, making this technology especially valuable for detecting pollutants at trace levels.[10] Nanopore technology also offers exceptional resolution, allowing for the simultaneous analysis of multiple analytes, including isomers, without the need for multiple instruments or coupling.[11] Furthermore, nanopore assays provide a wealth of information on analyte sizes,[12] shapes,[13]

Received: January 31, 2025
Revised: February 26, 2025
Accepted: March 12, 2025
Published: April 1, 2025

https://doi.org/10.1021/jacsau.5c00114
JACS Au 2025, 5, 1570−1590

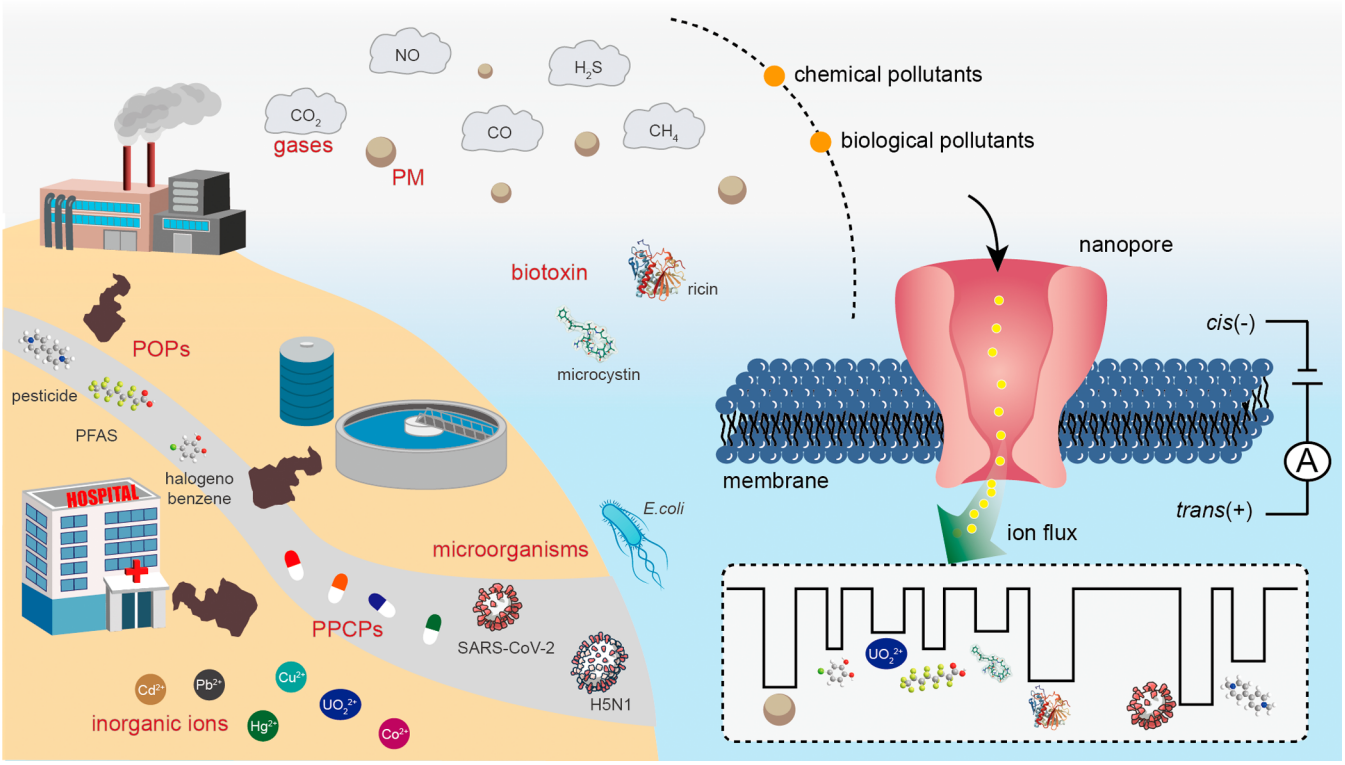

Figure 1. Scheme of environmental analysis using nanopore technology. Environmental matrices such as water, air, and soil contain complex mixtures of chemical and biological pollutants. Nanopore technology, with its broad detection range from single ions to microorganisms, offers the potential for the simultaneous detection of various environmental pollutants. As these pollutants pass through the nanopore, they generate current signals with distinct fingerprints, enabling rapid, multicomponent, and onsite environmental analysis.

charges,[14] conformations,[15] and host–guest interactions,[16] all of which are crucial for accurately identifying and characterizing pollutants, as well as understanding their toxicological effects. In addition, nanopore sensors are highly portable, making them ideal for onsite, real-time monitoring of pollutants in diverse and remote environments. The versatility of nanopore technology extends to its wide range of detection modes, enabling the analysis of various types of environmental pollutants, which is essential in addressing the growing diversity of contaminants. Recent advancements in small molecule detection have further enhanced the ability of these methods to analyze chemical pollutants.[17] Nanopore sequencing, a representative third-generation sequencing method, provides a powerful tool for analyzing microbial communities and environmental DNA.[18] Moreover, emerging developments in protein sequencing and carbohydrate analysis are expected to further accelerate the application of environmental multiomics.[19,20]

In this Perspective, we provide a comprehensive review of the environmental applications of nanopore technology. We begin by discussing various pollutants that are compatible with nanopore technology, focusing on chemical, and biological pollutants. Next, we categorize the current environmental efforts into two main areas: nanopore sensing-based pollutant analysis and nanopore sequencing-based microbiological analysis. In the first area, we separately introduce related studies using biological nanopores and solid-state nanopores, the two main types of nanopores. Diverse strategies have been introduced to inspire the design of excellent nanopore sensors that target more environmental pollutants. Subsequently, the advantages, methodologies and practical use of environmental microbial analysis using nanopore sequencing are reviewed in detail. Finally, we discuss the challenges and prospects of nanopore technologies in environmental monitoring, offering insights into their potential to address emerging environmental issues.

2. POLLUTANTS COMPATIBLE WITH NANOPORE TECHNOLOGY

Environmental pollutants are discharges of substances or energy into nature that cause acute or chronic damage to ecological balance and human health. According to their characteristics, pollutants can be classified as chemical, physical or biological.[21] Physical pollution refers to various forms of energy in the environment that exert deleterious effects on living organisms and their surroundings, such as heat, noise, light, and radiation. They are typically invisible and not detectable with nanopores. On the contrary, chemical and biological pollutants are more easily to be detected with nanopores. Key properties such as size, exposure level, solubility, volatility, and toxicity determine their potential for detection by nanopores. With a series of materials and techniques, nanopores have been fabricated with varying pore sizes, structures, and internal chemical environment,[22] targeting a broad scope of pollutants spanning ions, organic and inorganic small molecules, macromolecules, microorganisms and particles (Figure 1).

2.1. Chemical Pollutants

Chemical pollutants are prevalent in the environment and can be broadly categorized into inorganic pollutants (e.g., heavy metals, radionuclides, cyanides, carbon oxides, nitrogen oxides, halides, inorganic phosphides, inorganic sulfides and nano-

https://doi.org/10.1021/jacsau.5c00114
JACS Au 2025, 5, 1570−1590

Table 1. Detection of Pollutants with Biological Nanopore

Pollutant	Nanopore	Sensing Mechanism	LOD or Minimum Test Concentration	Citation
Zn^{2+}, Co^{2+}	α-HL $WT_6 4H_1$	Adapter-incorporated detection	50 nM (Zn^{2+})	36
Zn^{2+}, Co^{2+}, Cd^{2+}	α-HL $WT_6 4H_1$	Adapter-incorporated detection	240 nM (Zn^{2+}); 4.06 mM (Co^{2+}); 434 nM (Cd^{2+})	67
Au^{3+}	MspA D91M	Adapter-incorporated detection	0.2 μM	37
Au^{+}	MspA D91M	Adapter-incorporated detection	50 μM	68
Ca^{2+}, Mn^{2+}, Co^{2+}, Ni^{2+}, Zn^{2+}, Pb^{2+}, and Cd^{2+}	MspA D, MspA H	Adapter-incorporated detection	0.4 μM (Zn^{2+})	45
Ag^{+}	WT α-HL	Carrier-mediated detection	5 μM	70
Hg^{2+}	WT α-HL	Carrier-mediated detection	0.5 nM	82
Cu^{2+}	WT α-HL	Carrier-mediated detection	12 nM	71
Th^{4+}	WT α-HL	Carrier-mediated detection	0.45 nM	55
Pb^{2+}	WT α-HL	Reporter-triggered detection	4 nM	66
Cu^{2+}	WT α-HL	Carrier-mediated detection	16 nM	50
Cu^{2+}	α-HL $(M113N)_7$	Hybrid strategies	600 nM	59
Hg^{2+}	α-HL $(M113N)_7$	Hybrid strategies	25 nM	69
Zn^{2+}	WT α-HL	Reporter-triggered detection	100 nM	72
Fe^{3+}	α-HL $(M113N)_7$	Hybrid strategies	0.28 μM	73
Cu^{2+}	WT α-HL	Reporter-triggered detection	100 pM	65
UO_2^{2+}	α-HL $(M113F)_7$	Hybrid strategies	10 nM	56
halogeno benzene	MspA-PBA	Adapter-incorporated detection	0.1−2.24 mM	51
nitroaromatic	α-HL $(M113W)_7$, $(M113F)_7$, $(Met113Y)_7$	Adapter-incorporated detection	25 μm	41
omethoate	WT α-HL	Carrier-mediated detection	4.8 nM in solution and 100 ppb as vapor	27
paraquat	α-HL $(E111R/K147R)_7$	Carrier-mediated detection	2 nM (0.37 ppb)	61
PFPeA, PFHxA, PFHpA	WT aerolysin	Carrier-mediated detection	320 nm (PFPeA)	39
PFOA	WT α-HL	Carrier-mediated detection	40 μM	16
PFCAs and PFCSs	WT α-HL	Carrier-mediated detection	0.4−2 ppm	49
ampicillin	WT OmpF	Direct translocation	1 mM	38
gentamicin	PaMscS-V271I	Adapter-incorporated detection	5 mg/L	76
amoxicillin, azlocillin, and ampicillin	WT α-HL	Carrier-mediated detection	100 μM	74
ampicillin	WT α-HL	Carrier-mediated detection	100 μM	83
kanamycin	WT α-HL	Carrier-mediated detection	100 μM	42
microcystins (LR, RR, and YR)	WT α-HL	Direct translocation	0.25 μM	77
microcystins (LR, RR, and YR)	WT α-HL	Direct translocation	50 μg/L	79
AFB1, OTA, FB1	WT α-HL	Direct translocation	0.8 nM (AFB1), 0.45 nM (FB1), 1 nM (OTA)	78
ochratoxin	WT α-HL	Carrier-mediated detection	1.697 pmol/L	53
AFB1	WT α-HL	Reporter-triggered detection	0.54 pmoL/L	43
botulinum neurotoxins	WT aerolysin	Reporter-triggered detection	500 pM	84
Anthrax Lethal Factor	α-HL $(M113F)_7$	Hybrid strategies	15 nM	85
E. coli and *P. aeruginosa*	WT α-HL	Direct translocation	8×10^7 cfu/mL	44
Klebsiella pneumoniae	MspA	Carrier-mediated detection		80
influenza A	WT α-HL	Carrier-mediated detection		81

particles) and organic pollutants (e.g., hydrocarbons, organophosphorus compounds, organohalides, and organotin compounds). Water solubility is an important factor in nanopore sensing. Soluble pollutants, including most inorganic compounds, low-molecular-weight alcohols, ketones, aldehydes, and acids, are well suited for nanopore sensing. Slightly soluble pollutants, such as most polycyclic aromatic hydrocarbons and some nitrogen- or oxygen-containing organics, along with insoluble pollutants such as petroleum hydrocarbons and alkanes, pose challenges for detection. Methods such as cosolvents, temperature elevation, sonication, derivatization, or complexation (e.g., with cyclodextrins) can enhance water solubility.[23] Additionally, ionic liquid-based nanopore systems, which possess wide solubility properties, offer a promising approach to this challenge.[24,25] Pollutant volatility also needs to be considered. Nonvolatile pollutants are ideal for nanopore sensing, whereas gaseous or volatile organic pollutants (VOCs) may require specialized analyte delivery systems to bubbling the gases into the measurement buffer.[26−28] Another promising method involves using suitable adsorbents for selective

https://doi.org/10.1021/jacsau.5c00114
JACS Au 2025, 5, 1570−1590

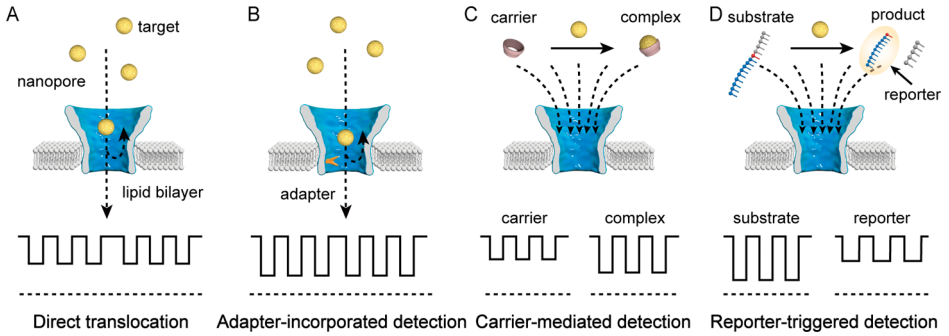

Figure 2. Different strategies for biological nanopore-based pollutant sensing. (A) Direct translocation: The target translocates through a wild-type nanopore, producing detectable current blockades. (B) Adapter-incorporated detection: The target reacts reversibly with an adapter engineered inside the nanopore, generating characteristic current blockades. (C) Carrier-mediated·detection: The target binds with a carrier outside the nanopore, resulting in distinct changes in current blockades compared with the presence of the carrier alone. (D) Reporter-triggered detection: The target triggers the production of a reporter, which induces specific current blockades that are different from those observed with the substrate alone.

adsorption of volatile compounds, followed by in situ desorption via heating or microwave-assisted techniques in the nanopore system.[29]

Persistent organic pollutants (POPs) are emerging pollutants that are resistant to degradation and tend to bioaccumulate. Listed by the Stockholm Convention, POPs include organochlorine pesticides, dioxins, polychlorinated biphenyls (PCBs), brominated flame retardants (BFRs), and per- and polyfluoroalkyl compounds (PFASs). Most POPs have low water solubility but high lipid solubility, making them easier to pass through cell membranes.[30] This presents challenges for artificial lipid bilayer-based nanopore detection systems.

As the use of pharmaceuticals and personal care products (PPCPs) continues to increase worldwide, PPCPs have been widely detected in the environment and have become a type of emerging pollutant. PPCPs can be divided into a wide variety of categories, including antibiotics, hormones, analgesics, steroids, eikonogens, spices, and preservatives. Most of these materials are highly polar and nonvolatile, making them suitable for nanopore detection. However, the residual concentrations of PPCPs are extremely low (ng/L), which places a high requirement on the sensitivity of nanopores.[31]

2.2. Biological Pollutants

Pathogenic microorganisms, drug-resistant microorganisms and their antibiotic resistance genes (ARGs) are the main microbial pollutants in the environment. Small organisms such as bacteria, viruses and prions may be analyzed directly with nanopore sensing, while gene-level species identification and ARG analysis can be performed using nanopore sequencing of DNA or RNA. Many byproducts from living organisms, particularly from industrial and agricultural processes, can accumulate in the environment and become pollutants. Among these byproducts, biotoxins, naturally occurring toxic substances, can enter the food chain and cause both acute and chronic poisoning. The chemical essence of toxins can be classified into small organic molecules (e.g., aflatoxins, fumonisins and ochratoxin A); peptides (e.g., mycotoxins, microcystins, conotoxins, and amanitin); proteins (e.g., botulinum toxin, diphtheria toxin, tetrodotoxin, and ricin); and lipopolysaccharides (e.g., lipid A, core polysaccharides, and O antigens). With the increasing application of nanopores in biological macromolecule fingerprinting, these biotoxins are potentially detectable using nanopores.

3. BIOLOGICAL NANOPORE-BASED SENSING FOR POLLUTANTS

Biological nanopores are a type of transmembrane protein with constriction diameters of 1−10 nm.[32] Their well-defined structures ensure reliable sensing performance, whereas their narrow pores and rich internal microenvironments provide high detection resolution, enabling the distinction of analogues,[33] homologues,[34] and isomers.[35] Through prokaryotic or eukaryotic expression, various transmembrane proteins with different structures have been developed as nanopores. Notable examples include *Staphylococcus aureus* alpha-hemolysin (α-HL),[36] *Mycobacterium smegmatis* porin A (MspA),[37] *E. coli* outer membrane protein F (OmpF),[38] *Aeromonas hydrophila* aerolysin,[39] and *Pseudomonas aeruginosa* mechanosensitive channel of small conductance (PaMscS).[40] These nanopores have been employed in the detection of various pollutants, including inorganic ions,[36] substituted benzenes,[41] POPs,[39] PPCPs,[42] biotoxins[43] and microorganisms[44] (Table 1). Four primary stochastic sensing strategies are employed: direct translocation, adapter-incorporated detection, carrier-mediated detection and reporter-triggered detection (Figure 3).

3.1. Sensing Methodologies

3.1.1. Direct Translocation. As natural transmembrane proteins, many biological nanopores serve as natural transport channels for specific substances, allowing direct sensing without additional modifications (Figure 2A). For example, OmpF facilitates the entry of β-lactam antibiotics into bacteria, and studies have shown that the Asp113, Glu117, Arg 42, Arg82 and Arg 132 residues in OmpF strongly interact with antibiotics such as ampicillin and penicillin, making them useful for sensing these compounds.[38] However, this strategy is currently limited to a very small fraction of polluting substances. Most pollutants interact too weakly with wild-type nanopores, causing them to pass through the pores too quickly to be effectively detected. While organisms possess a wide variety of transmembrane proteins, only a few have been isolated and used as nanopores. The screening of transmembrane proteins with specific functions is a promising strategy for developing novel biological nanopores.

3.1.2. Adapter-Incorporated Detection. The incorporation of adapters into biological nanopores can diversify their detection capabilities. These adapters bind specifically to target molecules, and their interactions slow the target's transport

https://doi.org/10.1021/jacsau.5c00114
JACS Au 2025, 5, 1570−1590

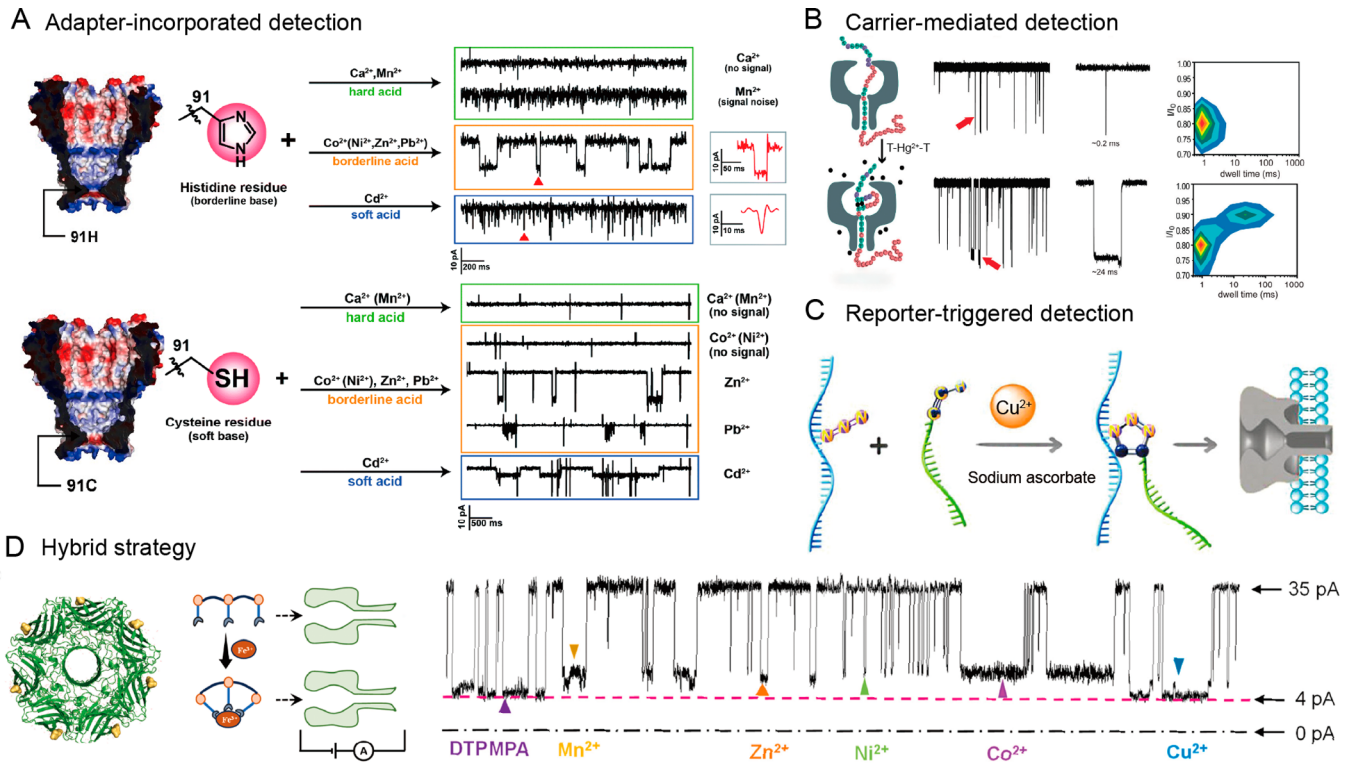

Figure 3. Heavy metal ion detection using biological nanopores. (A) Detection of various divalent metal ions using engineered MspA nanopores. Adapted with permission from ref 45. Available under a CC-BY 4.0 license. (B) Detection of Hg^{2+} using a wild-type α-HL nanopore with the assistance of a DNA carrier. Adapted from ref 52. Copyright 2011 American Chemical Society. (C) Cu^{2+} detection using a wild-type α-HL nanopore triggered by Cu^{2+}-induced click chemistry. Adapted from ref 65. Copyright 2019 American Chemical Society. (D) Sensing of different metal ions using a His-tagged α-HL $(M113\ K)_7$ nanopore assisted by an Fe^{3+} chelator. Adapted with permission from ref 73. Reproduced or adapted with permission from Elsevier.

through the pore, generating distinct current signatures (Figure 2B). Two methods are commonly used to integrate adapters. The first involves introducing natural amino acids with active groups into the pore constriction by site-specific mutation. For example, the introduction of imidazole-containing histidine or sulfhydryl-containing cysteine can be used to detect various heavy metal ions.[45] Frequently, α-HL and MspA are used as engineering templates. α-HL is a mushroom-shaped heptamer that has a vestibule with an opening of 4.8 nm in diameter and a stem with a constriction of 1.4 nm in diameter.[46] Compared with α-HL, MspA is a conical octamer with a smaller recognition region and is 1.2 nm in diameter and 0.6 nm in height.[47] Owing to its unique geometry, MspA provides a superior single-molecule sensing resolution.[37] To increase the signal consistency, nanopores can be further engineered with a single adapter by *in vitro* polymerization (for α-HL)[41] or prokaryotic coexpression (for MspA).[48] The second method involves the use of site-mutated amino acids as a bridge to further functionalize the pore in a covalent reaction manner. In this way, some organics, such as cyclodextrin (CD), porphyrin and phenylboronic acid, are immobilized in the pore constriction for the sensing of PFAS,[49] Cu^{2+},[50] and substituted benzene,[51] respectively.

3.1.3. Carrier-Mediated Detection. To avoid the complexity of pore engineering, molecules that can bind to a target can also be introduced as carriers outside the pore. When the carrier forms a complex with the target through affinity interactions or chemical coupling, the complex generates a distinct electrical signal due to configuration changes, differentiating it from the signal of the carrier alone (Figure 2C). This strategy is widely used in the detection of pollutants because of its simplicity, high sensitivity, and broad applicability. Typically, molecular carriers are large molecules that are easily detectable in nanopores. They can be biological recognition elements such as nucleic acid, peptides and proteins. Nucleic acids, with their flexible sequence design, have been programmed to target various ions, antibiotics pesticides and biotoxins.[27,42,52,53] Peptides and proteins, containing functional groups in their amino acid side chains (e.g., hydroxyl, carboxyl, sulfhydryl, and amino groups) and featuring distinct tertiary structures, enable specific interactions with a broad range of pollutants. Peptide carriers have been used for the detection of Cu^{2+},[54] Th^{4+},[55] and UO_2^{2+},[56] while protein carriers, such as zinc fingers, have been utilized for detecting Zn^{2+},[57] and calmodulin for detecting Ca^{2+}.[58] Macrocyclic molecules, such as CD[59,60] and calixarene,[61] crown ethers,[62] cucurbiturils[63] and emiaza-bambusurils,[64] fit well inside most nanopores and are thus also used as molecular carriers. Their unique hydrophilic and hydrophobic properties, along with modifiable internal ring walls, make them promising for detecting a wide range of analytes.

3.1.4. Reporter-Triggered Detection. In this strategy, the target is not directly involved in the sensing of the biological nanopore. Instead, it triggers a detectable reporter molecule through chemical reactions (Figure 2D). As the reporter molecule passes through the nanopore, it generates a characteristic electrical signal, thereby indirectly sensing the target. Catalytic reactions are most commonly used, as pollutants such as heavy metal ions often act as cofactors in

https://doi.org/10.1021/jacsau.5c00114
JACS Au 2025, 5, 1570−1590

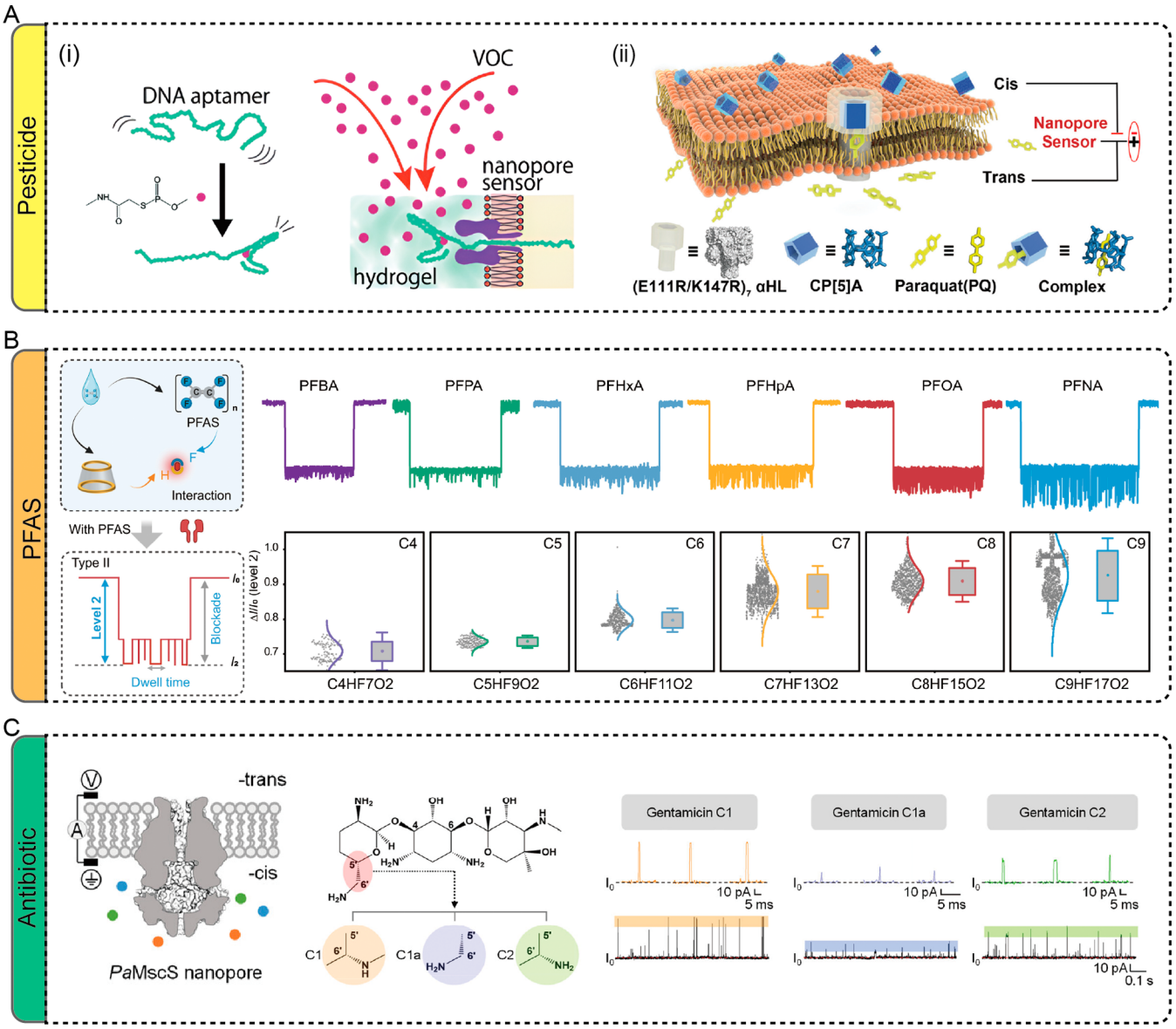

Figure 4. POP and PPCP detection with biological nanopores. (A) Detection of pesticides (e.g., omethoate (i) and paraquat (ii)) using α-HL nanopores. (i) Adapted with permission from ref 27. Reproduced or adapted with permission from The Royal Society of Chemistry. (ii) Adapted with permission from ref 61. Reproduced or adapted with permission from The Royal Society of Chemistry. (B) PFAS detection using an α-HL nanopore assisted by γ-CD. Adapted with permission from ref 49. Copyright 2024 the American Association for the Advancement of Science. (C) Gentamicin detection with a mutated PaMscS nanopore. Adapted from ref 76. Copyright 2024 American Chemical Society.

catalytic reactions, such as Cu^{2+}-catalyzed click reactions[65] and Pb^{2+}-catalyzed DNA cleavage.[66]

3.2. Environmental Applications

3.2.1. Inorganic Ions. Nanopores are widely used for detecting heavy metal ions[7] and radioactive ions,[56] although direct translocation detection is rare because of the small size of these ions. The other three strategies mentioned above or their hybrids are typically employed. In adapter-incorporated detection, specific amino acids are introduced into pore recognition sites to capture target ions. For example, Hagan Bayley et al. engineered α-HL with histidine to recognize Cd^{2+}, Zn^{2+}, and Co^{2+} at the nanomolar level.[67] Shuo Huang et al. developed a series of MspA mutants for the improved detection of various heavy metal ions, including Au^{+}, Au^{3+}, Ca^{2+}, Mn^{2+}, Co^{2+}, Ni^{2+}, Zn^{2+} and Pb^{2+} (Figure 3A).[37,45,68] Carrier-mediated detection often uses DNA with specific sequences that bind heavy metal ions such as Hg^{2+},[52] Pb^{2+},[69] Ba^{2+},[69] or Ag^{+},[70] thereby prolonging the translocation time for detection (Figure 3B). Peptides,[54] proteins,[55] CD,[71] and porphyrins[50] have also been reported as carriers for the sensing of Cu^{2+}, Th^{4+} and Zn^{2+}. Reporter-triggered detection employs the catalytic activity of metal ions, such as the Cu^{2+}-induced ligation of ssDNAs to form forked DNA, producing unique current signatures (Figure 3C).[65] $Pb^{2+}$and Zn^{2+} have also been detected by activating enzyme digestion of DNA[66] and peptides,[72] respectively. Hybrid strategies combine these methods, where the nanopore is engineered to enhance the interaction between the pore and a carrier or reporter. Xiyun Guan utilized an engineered α-HL and an Fe^{3+} chelation agent as a carrier to detect Fe^{3+} with a detection limit of 0.28 μM (Figure 3D)[73] and used a similar strategy to detect UO_2^{2+} ions[56] at nanomolar concentrations with high selectivity.

https://doi.org/10.1021/jacsau.5c00114
JACS Au 2025, 5, 1570−1590

Table 2. Detection of Pollutants with Solid-State Nanopores

Pollutant	Nanopore	Pore Diameter	Output Signal	LOD or Minimum Test Concentration	Citation
Zn^{2+}	PET	7−45 nm	ICR	10 μM	125
Hg^{2+} and Ag^{+}	alumina	15 ± 4 nm	ICR	1 nM	114
Cr^{3+}	PET	63 nm	ICR	16 nM	116
Cu^{2+}	PET	10 nm	ICR	3.37×10^{-10} μM	149
Fe^{3+}	PET	10 nm	ICR	10^{-3} nM	120
Pb^{2+}	PET	60 nm	ICR	10^{-15} M	110
multivalent metal ions	glass	80 nm	ICR	10^{-18} M	126
La^{3+}	PET	63 nm	ICR	5 nM	122
Hg^{2+}	PET	30 nm	ICR	8 nM	112
Cs^{+}	PET	20 nm	ICR	100 μM	123
Ce^{3+}	PET	200 nm	ICR	1 nM	121
uranyl ion	PI	9 nm	ICR	1 fM	124
phosphonates	PET	30 nm	ICR	27 nM (2-aminoethylphosphonate)	128
carbonate	PI	20 nm	ICR	0.02 M	131
Cl^{-}	PI	8−11 nm	ICR	10 μM	132
F^{-}	PI	10 nm	ICR	0.01 nM	129
paraquat and diquat	glass	72 nm	ICR	0.034 nM (paraquat)	100
tetracycline	Si_3N_4	8−9 nm	RPS	2 ng/mL	101
ibuprofen and sulfamethoxazole	SiN_x	2.4−14.5 nm	RPS	21 μg/L (ibuprofen); 12 μg/L (sulfamethoxazole)	134
CO_2	PI	9 nm	ICR		136
NO	PET	23 nm	ICR	0.1 μM	138
HCHO	PET	30 nm	ICR	10^{-9} mg/mL	137
CO	PET	18 nm	ICR	0.1 μM	139
ricin	PET	4 nm	ICR	100 nM	103
ricin	glass	56 nm	RPS	2.8 nM	140
MC-LR	SiN_x	10−20 nm	RPS	0.1 nM	141
okadaic acid	SiN_x	3−4 nm	RPS	0.03 pg/mL	142
filamentous virus	SiN	12−50 nm	RPS	0.02 mg/mL (1 nM)	143
tobacco mosaic virus	SiN	20, 30, 50 nm	RPS		144
influenza A (H1N1 and H3N2), influenza B	Si_3N_4	300 nm	RPS		150
four types of coronaviruses	SiN	300 nm	RPS	2.5 pfu/μL	147
A (H1N1) and B	Si_3N_4	300 nm	RPS		146
cedar and cypress pollens	Si_3N_4	50 nm	RPS	1 mg/mL	105
dirt particulates	SiN	14 nm	RPS		148

3.2.2. Substituted Benzene. Substituted benzene pollutants are compounds with one or more active groups attached to a benzene ring. These include halogenated benzenes, nitrobenzenes, aminobenzenes, and phenols, which are commonly used in industry and are known for their environmental toxicity. The benzene rings and active groups of these materials can be used to establish interactions with nanopores. Through aromatic−aromatic interactions, Hagan Bayley et al. detected six nitrobenzenes by introducing aromatic residues (e.g., Phe, Tyr, or Trp) at site 113 in α-HL, which is promising for detecting various aromatic pollutants.[41] Shuo Huang et al. engineered an MspA nanopore with a sole phenylboronic acid to distinguish halophenol homologues differing only in their halogen atoms and substitution positions, demonstrating the high resolution of MspA in small-molecule sensing.[51]

3.2.3. POPs. Pesticides and per- and polyfluoroalkyl substances (PFASs) are typical POPs that are detected using biological nanopores.[27,49,61] Shoji Takeuchi et al. developed a pesticide vapor sensor using hydrogel droplets to absorb VOCs, successfully detecting omethoate at 100 ppb with a DNA aptamer (Figure 4A).[27] This platform overcomes the limitations of nanopores to nonvolatile compounds. Junqiu Liu et al. detected paraquat using an α-HL mutant and carboxyatopillar [5] arene, achieving a detection limit of 0.37 ppb (Figure 4A).[61] PFASs are highly fluorinated aliphatic compounds with a CF_2 unit backbone and have become a major focus of environmental research because of their potential health risks. Kaipei Qiu et al. first used wild-type aerolysin to discriminate three short-chain PFASs, but the target PFASs are required to be chemically ligated to a cationic peptide for enhanced capture and retention within the nanopore.[39] Chang Liu et al. directly identified homologues of the perfluoroalkyl carboxylic acid (PFOS) and perfluoroalkyl sulfonic acid (PFOS) families through host−guest interactions between cyclodextrin and FPASs (Figure 4B).[49] The binding of PFASs to human serum albumin has been monitored in real time, providing a single-molecule tool to study the toxicity of pollutants to biomolecules.[16]

3.2.4. PPCPs. Among PPCPs, antibiotics contribute to the rise of antibiotic-resistant bacteria, which poses a global public health issue. Since Sergey M. Bezrukov et al. first reported ampicillin transport through OmpF,[38] various antibiotics, such as amoxicillin,[74] kanamycin,[42] and digoxigenin[75] have been detected using DNA- or CD-assisted nanopore sensing. Recently, Jia Geng et al. used a mutated PaMscS nanopore to rapidly detect gentamicin (10 nM−10 μM) in blood and developed a continuous monitoring device for point-of-care monitoring of small molecules in biofluids (Figure 4C).[76] This

https://doi.org/10.1021/jacsau.5c00114
JACS Au 2025, 5, 1570−1590

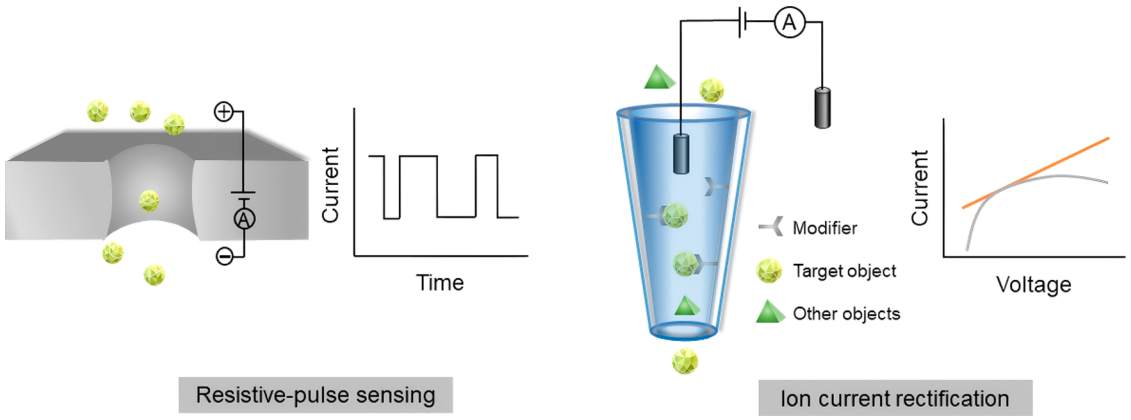

Figure 5. Different detection modes of solid-state nanopore-based biosensing.

research demonstrates the advantages of nanopores for onsite and real-time pollutant monitoring.

3.2.5. Biotoxins. Biotoxins range from small molecules to biomolecules. Some small-molecule biotoxins, such as aflatoxin B1 (AFB1), ochratoxin A (OTA) and fumonisin B1 (FB1), can interact with biological nanopores, enabling rapid detection through direct translocation.[77] Claudio Gabriel Rodrigues et al. used α-HL to distinguish these mycotoxins, achieving nanomolar-level detection by adjusting the KCl concentration.[78] The enhanced detection specificity and sensitivity of these mycotoxins were also achieved via the use of DNA aptamers.[43] Additionally, peptide and protein biotoxins, such as microcystins (e.g., MC-LR, MC-RR, and MC-YR), have been differentiated using a α-HL nanopore, highlighting the high resolution of biological nanopores in detecting similar toxin variants.[79]

3.2.6. Microorganisms. Tudor Luchian et al. first reported the detection of *E. coli* and *P. aeruginosa* at the single-particle level by using electrostatic interactions to drive negatively charged bacteria into collisions with α-HL.[44] However, due to their significant size differences, direct sensing of microorganisms with biological nanopores is rare. Instead, biological nanopores are useful for the indirect detection of microorganisms by identifying related substances such as genetic material. DNA probes targeting 16S rRNA or viral promoter regions have been respectively used to identify *Klebsiella pneumoniae*[80] and influenza A viruses,[81] offering a rapid method of microbial identification without sequencing.

4. SOLID-STATE NANOPORE-BASED SENSING FOR POLLUTANTS

Solid-state nanopores are fabricated by milling nanometer-sized holes into thinned membranes supported on a substrate. A variety of materials have been used for these membranes, typically classified into categories such as silicon nitrides (SiN_x),[86] oxides (SiO_2,[87] TiO_2,[88] HfO_2,[89] Al_2O_3[90]), polymers (polyimide (PI)[91] or polyethylene terephthalate (PET)),[92] glass nanopipettes,[93] carbon nanotubes,[94] and 2D materials (graphene,[95] boron nitride,[96] molybdenum disulfide,[28] and transition metal carbides[97]). Many fabrication techniques are available to create nanopores with precise control, including focused electron beam/ion beam milling, dielectric breakdown, ion track etching, photochemical etching, anodization and laser pulling.[98] Solid-state nanopores offer controllable pore geometries and exhibit excellent mechanical, optical, thermal, and chemical stability, making them suitable for a wide range of analytes and conditions.[99] Functional modifications to their inner walls via chemical deposition, plating, or covalent grafting of organic molecules or biomolecules enable the detection of inorganic ions,[7] POPs,[100] PPCPs,[101] gases,[102] biotoxins,[103] microorganisms[104] and particulates (Table 2).[105] Two primary detection modes are used, including resistive-pulse sensing (RPS) and ion current rectification (ICR) sensing (Figure 5).

4.1. Detection Strategies

4.1.1. RPS. RPS operates based on the ionic current blockade caused by analytes translocating through the orifice of a solid-state nanopore, enabling single-molecule detection. When an analyte passes through or partially obstructs the nanopore, it causes a reversible change in the ionic current, generating a current "pulse" or blockade. The duration and depth of these pulses provide detailed information about the analyte's size, charge and other properties, whereas the frequency of these pulses reveals the analyte's concentration (Figure 5). Compared with biological nanopores, solid-state nanopores face challenges in terms of the signal-to-noise ratio and fabrication reproducibility, especially for small nanopores with sizes of a few nanometers. As a result, RPS is more commonly used for detecting larger contaminants such as biomacromolecules,[106] microorganisms[107] and PMs,[105] which can significantly block nanopores through volume exclusion.

4.1.2. ICR. Solid-state nanopore-based pollutant analysis predominantly employs ICR sensing, where the characteristic asymmetric current–voltage (I–V) curves are modulated by analyte-induced changes in the nanopore surface. ICR often occurs in asymmetric nanopores (such as conical PET nanopores) and manifests as an asymmetric I–V curve. This is primarily caused by the interaction between the asymmetric electric double layer (EDL) on the pore wall and the electrolyte ions, which results in the asymmetric migration of cations and anions.[108] The presence of an analyte can alter the surface charge or configuration of the nanopore, which affects the EDL and ion transport properties, resulting in a change in the I–V curve (Figure 5). The rectification ratio, which is defined as the ratio of the currents measured at two equal but opposite applied potentials, provides information about analyte identities and concentrations. ICR sensing is faster than RPS but lacks the ability to observe single-molecule events, which makes it less suitable for simultaneous multitarget analysis. Another drawback of ICR sensing is that it requires regeneration of the sensor with a stronger chelating agent after each measurement.[109]

https://doi.org/10.1021/jacsau.5c00114
JACS Au 2025, 5, 1570–1590

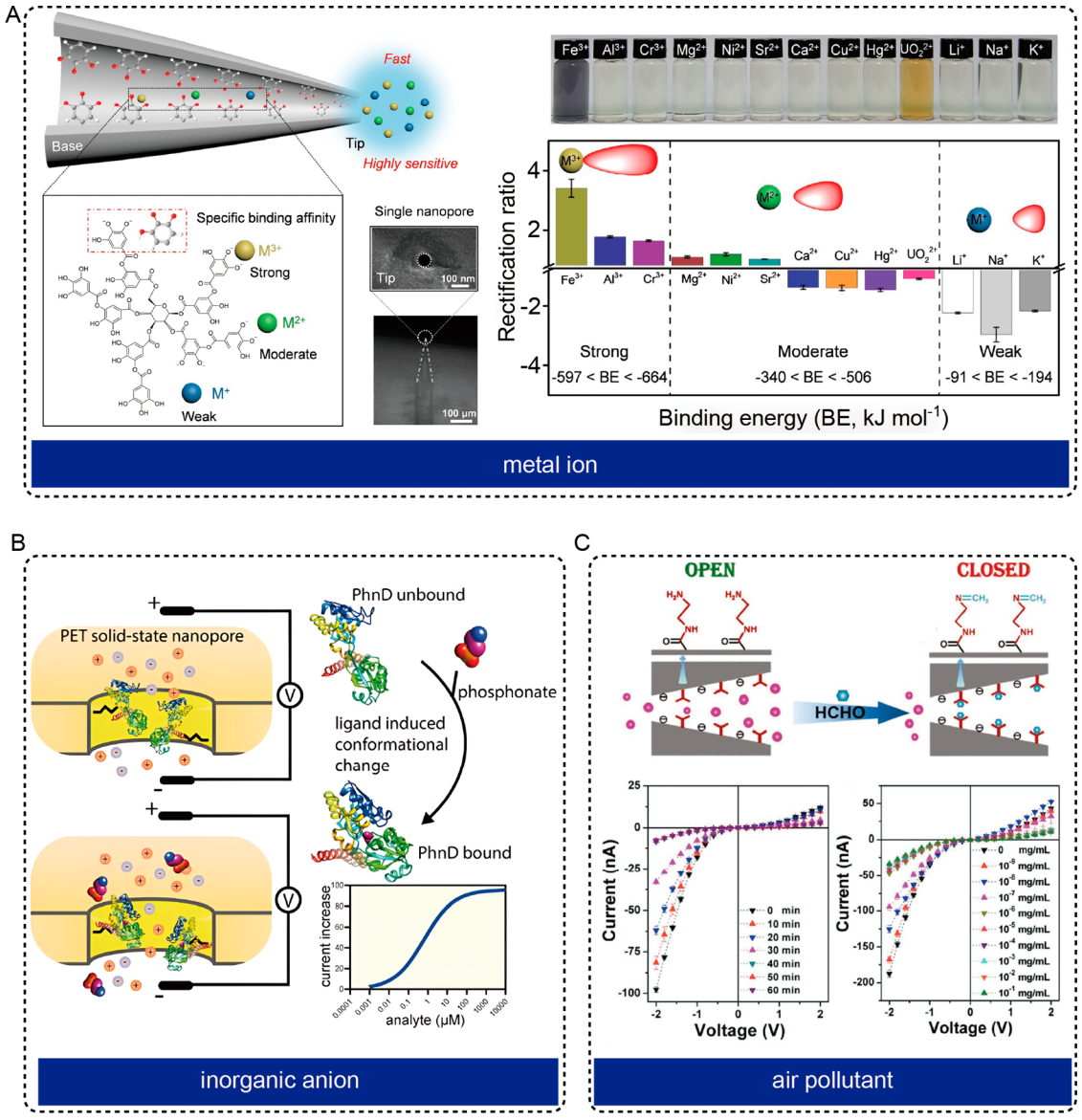

Figure 6. Examples of environmental pollutant detection using ICR sensing. (A) TA-modified PET nanopores for multivalent metal ion detection. Adapted with permission from ref (126). Reproduced or adapted with permission from Elsevier. (B) Phosphonate-binding protein PhnD-modified PE'T nanopores for phosphate detection. Adapted with permission from ref (128). Copyright 2019 American Chemical Society. (C)EDA-functionalized nanopore for HCHO detection. Adapted with permission from ref (137). Reproduced or adapted with permission from John Wiley and Sons.

4.2. Environmental Applications

4.2.1. Inorganic Ions. Solid-state nanopores are widely used for sensing a variety of inorganic ions, including metal ions and inorganic anions. The metal ions detected in these nanopores include heavy metal ions (e.g., Pb^{2+},[110,111] Hg^{2+},[112−115] Cr^{3+},[116] Cu^{2+},[117] Zn^{2+},[118] Ag^{+},[114,119] and Fe^{3+},[120]); rare earth metal ions (e.g., Ce^{3+}[121] and La^{3+}[122]); alkali metal ions (Cs^{+}[123]) and radioactive metal ions (UO_2^{2+}[124]). ICR sensing using PET or PI nanopores is the primary strategy for detecting these metal ions. PET nanopores are modified with adapters such as macrocyclic molecules,[123] DNA,[112] or peptides[125] to selectively capture one or two types of target metal ions. This high specificity is advantageous for analyzing complex environmental samples. For example, UO_2^{2+} in real seawater can be detected using a PI nanopore functionalized with 4-amino benzamidoxime (ABX) owing to the specific binding capability of amidoxime groups with UO_2^{2+}.[124] Notably, Jyh-Ping Hsu et al. developed tannic acid (TA)-modified PET nanopores for multivalent metal ion detection, employing different binding affinities between trihydroxy phenolic groups and different metal ions (Figure 6A).[126] In addition to binding with nanopores, metal ions such as Pb^{2+}[111] or Zn^{2+}[127] can also be indirectly detected by activating the DNAzyme to cleave the DNA substrate modified on the pore wall, which results in changes in the I−V curve. Like metal ions, inorganic anions are typically detected using ICR. Bodo Laube et al. used a PET nanopore modified with the phosphonate-binding protein PhnD to sense 2-amino-ethylphosphonic acid and ethylphosphonate (Figure 6B).[128] This strategy has also been employed to detect F^{-},[129,130] CO_3^{2-},[131] Cl^{-}[132] and PO_4^{2-}.[133]

4.2.2. POPs. Solid-state nanopores have been employed to detect pesticides through host−guest interactions between cylindrarenes and pesticides.[100] When pesticides bind to a

https://doi.org/10.1021/jacsau.5c00114
JACS Au 2025, 5, 1570−1590

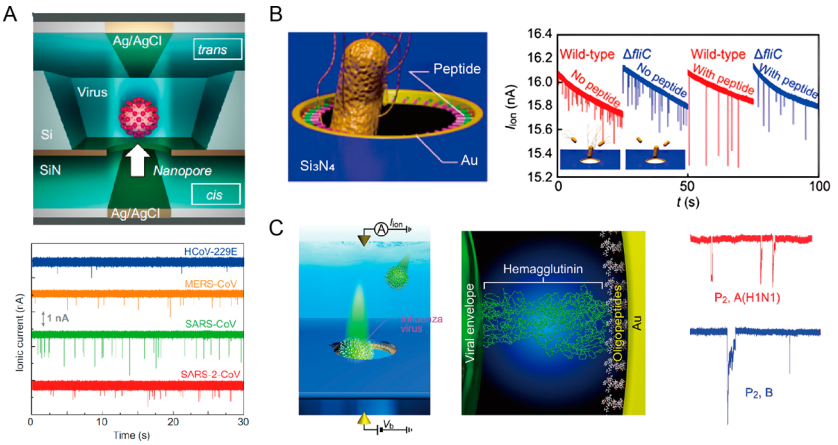

Figure 7. Microorganism detection via the RSC. (A) Direct translocation of microorganisms through a SiN nanopore for distinguishing coronaviruses of similar size. Adapted with permission from ref 147. Available under a CC-BY 4.0 license. (B) Discrimination of wild-type *E. coli* and a flagellin-deletion mutant using a peptide-functionalized solid-state nanopore. Adapted from ref 145. Copyright 2018 American Chemical Society. (C) Discrimination of influenza viruses with an oligopeptide-functionalized solid-state nanopore. Adapted from ref 146. Copyright 2018 American Chemical Society.

cylindrarenes-modified nanopipette, the charge on the pore wall shifts from negative to positive, significantly altering the ICR ratio. By adjusting the cavity size of cylindrarenes, different pesticides can be selectively detected. The sensitivity was enhanced by further incorporating gold nanoparticles (AuNPs) into the nanopipette, achieving a detection limit for paraquat as low as 0.73 nM. These nanopipettes successfully detected pesticide residues in river water, apples and tea, demonstrating their potential for real-world applications.

4.2.3. PPCPs. The detection of PPCPs using solid-state nanopores typically relies on RPS. Since most PPCPs have small molecular diameters (~1 nm), a carrier is often needed to generate a detectable signal. Proteins, owing to their larger sizes and affinity for many PPCPs, serve as ideal carriers. Protein−drug interactions enable single-molecule detection of various PPCPs, such as tetracycline,[101] ibuprofen, and sulfamethoxazole,[134] as the protein−drug complex passing through the solid-state nanopore generates distinct current signals. This strategy is highly selective and sensitive but requires the binding of PPCPs and proteins to induce significant structural changes.

4.2.4. Greenhouse Gases and Harmful Gases. Greenhouse gases (e.g., CO_2 and CH_4) and harmful gases (e.g., CO, NO_x, SO_2, NH_3, O_3 and VOCs) are major air pollutants that degrade air quality and contribute to climate change. While nanopore sensors are typically used in aqueous environments, solid-state nanopores have also been employed for gas detection. By bubbling target gases into a buffer solution, small-molecule functionalized solid-state nanopores have been used to detect gases such as CO_2,[135,136] HCHO,[137] NO,[26,102,138] and CO[139] using ICR sensing. For example, HCHO can be detected through a nucleophilic addition reaction with ethanediamine (EDA) immobilized on nanochannels, achieving a detection limit as low as 10^{-9} mg/mL (Figure 6C).[137] This functionalized nanopore has also been successfully used to identify HCHO in rooms and seafood. However, irreversible covalent interactions make the sensor unsuitable for repeated use. A reversible interaction could offer a better balance between high specificity and recyclability.

4.2.5. Biotoxins. There are two main strategies for biotoxin detection using solid-state nanopores. The first involves functionalizing the nanopore with adapters to capture biotoxins directly. In this way, Charles R. Martin[103] and Li-Qun Gu[140] successfully detected ricin using nanopores modified with antibodies and RNA aptamers, respectively. The second strategy uses carriers to bind with the target biotoxin, forming a complex that generates detectable current pulses when passing through the pore. Deqiang Wang et al. designed aptamer-conjugated AuNPs for detecting MC-LR with an SiN_x nanopore.[141] They also developed a similar method using aptamer-conjugated magnetic beads to detect okadaic acid, with a detection limit of 0.03 pg/mL.[142]

4.2.6. Microorganisms. Solid-state nanopores have adjustable sizes across a high dynamic range and are ideal for single-particle detection of microorganisms. To allow microorganisms to pass through pores, solid-state pores with diameters greater than 10 nm, and in some cases up to 300 nm, are needed. Direct translocation of pathogenic microorganisms through large-sized solid-state nanopores has been used to detect stiff filamentous viruses,[143] tobacco mosaic viruses,[144] *E. coli*[145] and *Bacillus subtilis*.[107] Four coronaviruses have also been distinguished with high sensitivity, enabling the detection of ARS-CoV-2 in saliva within 5 min (Figure 7A). To further enhance the selectivity, Au nanopores modified with peptides that recognize specific microbial surface characteristics, such as flagella (Figure 7B)[145] or hemeagglutinin (Figure 7C),[146] have been constructed to distinguish similar species. Machine learning methods are also employed to analyze multiple features of translocation signals, facilitating the detection of various bacteria and viruses for biological risk monitoring.[147]

4.2.7. PM. PM including dust, smoke, and pollen is a major air pollutant that harms the cardiovascular and respiratory systems and disrupts meteorological and chemical processes. Owing to the large size of PMs, solid-state nanopores enable direct sensing of PMs, providing insights into their size, shape, and surface charge. Tomoji Kawai et al. used a Si_3N_4 nanopore to distinguish between cypress and cedar pollen with 92% accuracy using machine learning.[105] Marija Drndić et al. employed an SiN nanopore to detect Antarctic dirt particulates and estimate the average diameter of particles according to their degree of blockage.[148]

https://doi.org/10.1021/jacsau.5c00114
JACS Au 2025, 5, 1570−1590

5. NANOPORE SEQUENCING FOR ENVIRONMENTAL MICROBIAL ANALYSIS

Microorganisms are the most abundant and diverse life forms on Earth. They play essential roles in biochemical cycles and ecological remediation but can also cause environmental pollution and spread infectious diseases. A comprehensive characterization of microbial communities is crucial for environmental protection and disease surveillance. Traditional microbial culture techniques, which provide valuable insights, are limited because less than 1% of microorganisms can be cultured in laboratories due to their complex growth requirements.[151] High-throughput sequencing (HTS) technologies such as Illumina have revolutionized microbiome research by enabling direct amplicon sequencing, metagenomic sequencing and whole-genome sequencing, providing insights into microbiome diversity, population structures and evolution.[152] However, HTS is limited by short read lengths (50−350 bp), which make it difficult to analyze complex regions such as structural variants and repetitive sequences, leading to incomplete genome assemblies. This also complicates the taxonomic classification and genome assembly of closely related species. As a frontier in third-generation sequencing technology, nanopore long-read sequencing offers a promising alternative by providing access to previously inaccessible genomic regions.[153]

5.1. Overview of Nanopore Sequencing Technology

The concept of nanopore sequencing dates back to the 1990s, with a patent filed by George Church et al. in 1995.[154] In this technique, single-strand DNA or RNA is translocated through a nanopore by a motor protein, and changes in the ionic current are used to decode the nucleic acid sequence.[154] In 2014, Oxford Nanopore Technologies (ONT) commercialized nanopore sequencing with the MinION device, a compact and portable platform containing 512 nanopore channels. The latest versions of MinION (flow cell R9.4.1 and R 10.4.1) achieve 99% accuracy with sequencing speeds of up to 450 bases per second by utilizing a mutant Curlin sigma S-dependent growth subunit G (CsgG) from *E. coli* and an engineered helicase that has not been identified (Figure 8).[155,156]

ONT sequencing has brought significant advantages to the field of environmental microbiome research.[135] (i) Its ability to generate extremely long reads, up to 2.4 M, surpasses other platforms such as Illumina NovaSeq (>10 kb) and PacBio (5−70 kb), simplifying genome assembly and enabling species-level microbial profiling.[157] (ii) ONT also enables native DNA and RNA sequencing without amplification, offering more complete characterizations across the genomic, transcriptomic, and epigenomic levels.[158] (iii) ONT allows real-time surveillance of pathogenic microorganisms, with MinKNOW software converting read current data into nucleotide sequences, while the ReadUntil API expels nontarget molecules.[159] (iv) The portability of MinION, which weighs only 90 g, combined with the automated VolTRAX library preparation system, makes it powerful for onsite sequencing, even in extreme environments such as the Antarctic Dry Valleys,[160] the Canadian High Arctic,[161] the largest European ice cap[162] or the International Space Station.[163]

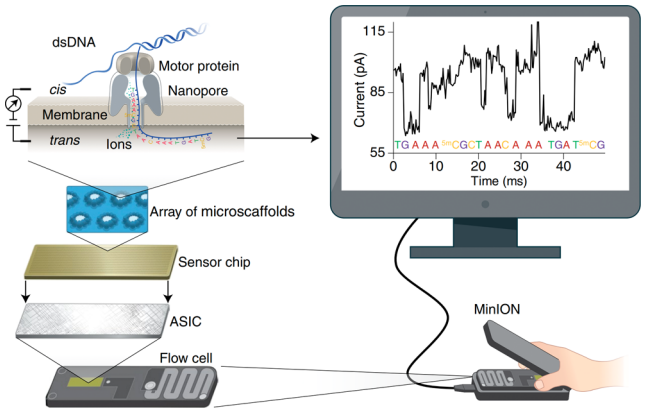

Figure 8. Principle of nanopore sequencing. Adapted with permission from ref 155. Reproduced or adapted with permission from Springer Nature.

5.2. Nanopore Sequencing Methodologies

5.2.1. Targeted Sequencing. Targeted sequencing, namely, amplicon sequencing, refers to the analysis of regions of interest (ROIs) within a genome. Compared with whole-genome sequencing, targeted sequencing is more cost-effective and offers faster sequencing and analysis speeds. Targeted sequencing of the ribosome RNA operon (rrn operon) region is widely used as the gold standard marker for microorganism community profiling (Table 3).[164] The key taxonomic markers within this region include the 16S rRNA gene (1,500 bp) for bacteria and archaea, the 18S rRNA gene (1,800−2,000 bp) for eukaryotes, and the internal transcribed spacer gene (ITS, 450−700 bp) for fungi. For example, the bacterial 16S rRNA gene contains nine hypervariable regions (V1 to V9) that show sequence variations across bacterial species that are separated by highly conserved sequences. Due to the short-read lengths of NGS, only partial variable regions of marker genes can be analyzed using conserved region-targeted PCR primers.[165] Long-read ONT sequencing platforms enable full-length sequencing of rRNA genes, such as the 16S rRNA gene,[166] 18S rRNA gene,[167] or entire rrn operons (e.g., 16S-ITS-23S for bacteria and 18S-ITS-28S for fungi),[168] providing higher taxonomic resolution (Figure 9). Zhang et al. evaluated the performance of the latest Oxford PromethION device for full-length 16S amplicon sequencing from both mock microbial communities and environmental samples, achieving an average accuracy of 99.42% and species-level identification surpassing the resolution of short-read sequencing.[166] Furthermore, ONT is the only platform that supports direct RNA sequencing, allowing for full-length 16S rRNA sequencing without the need for reverse transcription or amplification, thus avoiding biases related to reverse transcriptase activity and providing valuable insights into RNA epigenetics.[169]

5.2.2. Shotgun Sequencing. Shotgun sequencing involves randomly fragmenting the genome into small DNA pieces, which are then individually sequenced and reassembled to reconstruct the original genome (Table 3). This approach has been applied to sequence the genomic DNA (gDNA) of isolated species (whole-genome sequencing) or the total gDNA of microbial communities (metagenomic sequencing), offering deeper insights into microbial diversity, population structures, functional roles and the relationships between microorganisms and their environment.[170] Owing to its long read lengths, ONT sequencing is well suited for shotgun sequencing, significantly improving the continuity of genome assembly (Figure 9). Long reads help resolve complex genomic structures and identify bacterial pathogenicity islands (PAIs),

https://doi.org/10.1021/jacsau.5c00114
JACS Au 2025, 5, 1570−1590

Table 3. Nanopore Sequencing for Environmental Microbial Analysis

Sequencing Methodologies	Microbial Species	Application	Instrument	Matrices	Citation
Targeted sequencing	Poliovirus	Pathogenic microorganism surveillance	MinION Mk1B R9.4 flow cell	feces and wastewater	171
	SARS-CoV-2	Pathogenic microorganism surveillance	R10.4.1 flow cell	wastewater	172
	Hepatitis E Virus and Norovirus	Pathogenic microorganism surveillance	MinION R9.4.1 flow cell	wastewater	173
	Escherichia coli, *Klebsiella pneumonia*, and *Haemophilus influenzae*	Antibiotic-resistant microorganism analysis	MinION FLO-MIN106 R9.4.1 flow cell	feces	174
	Alcanivorax	Functional microorganism analysis	MinION R9.4.1. flow cell	seawater	175
Shotgun sequencing (whole-genome sequencing)	SARS-CoV-2	Pathogenic microorganism surveillance	MinION Mk1b R9.4.1 flow cell	wastewater	176
	Influenza A viruses	Pathogenic microorganism surveillance	GridION FLO-MIN106D R9 flow cell	wastewater	177
	Brevibacterium	Functional microorganism analysis		wastewater	178
	Shewanella decolorationis	Functional microorganism analysis	MinION FLO-MINSP6 flow cell	wastewater	179
Shotgun sequencing (metagenomic sequencing)	*Bacillus subtilis* and *Escherichia coli*	Pathogenic microorganism surveillance	MinION FLO-MIN 106D R9.4.1 flow cell	feces	180
	Bacillus haynesii	Pathogenic microorganism surveillance	MinION flow cell	soil	181
	Thermophilic anaerobic digestion microbiome	Functional microorganism analysis	GridION	food waste and sludge	182
	Potential POP-degrading microbiome	Functional microorganism analysis	GridION SpotON R9.4 flow cell	soil	183
	Proteobacteria, *Firmicutes*, and *Bacteroidetes*	Functional microorganism analysis	MinION	lake sediment	184

which encode virulence factors. However, ONT sequencing is prone to insertion and deletion errors, affecting its accuracy.[185] To overcome this, a hybrid assembly strategy combining ONT and Illumina sequencing is widely used, in which ONT sequencing provides long-read fragments for assembly and Illumina sequencing refines and corrects the results.[186] By polishing ONT long-read assemblies with short-read data, Singleton et al. successfully generated 1,083 high-quality prokaryotic genomes from 23 sewage sludge samples.[187] Although effective in correcting frame-shift errors, this approach is computationally intensive, increasing both cost and complexity. With increased accuracy, recent advances in the use of Oxford Nanopore R10.4 have resulted in near-finished microbial genomes without short-read polishing, benefiting research in biodiversity assessments, functional gene annotation and ARG profiling.[185]

5.3. Environmental Applications

5.3.1. Pathogenic Microorganism Surveillance. Pathogens that are responsible for infectious diseases pose significant biosecurity threats and require prompt detection because of their rapid spread and evolution.[188] Nanopore target sequencing enables rapid, real-time DNA sequencing, making it increasingly effective for identifying and monitoring bacterial and viral pathogens in environmental samples, including air,[189] building dust,[190] freshwater,[191] faeces,[180] soil[181] and especially wastewater.[176] Wastewater, as a routine byproduct of human activities, provides invaluable insights into community health. ONT devices have been widely used in wastewater-based epidemiology (WBE) research for monitoring pathogens such as poliovirus,[171] Ebola virus,[192] monkeypox virus,[193] SARS-CoV-2,[172] hepatitis E virus,[173] norovirus[173] and avian influenza,[177] offering significant advantages in terms of reduced turnaround time and improved cost-effectiveness. With the latest ONT platform, R10.4.1, nanopore sequencing achieves >99% accuracy for single nucleotide variants (SNVs) and insertions/deletions (indels) in viral genes, providing high-resolution insights into the temporal dynamics of SARS-CoV-2 variants in wastewater.[172] Additionally, the portability of the nanopore sequencing platform allows for onsite operation, even in extreme environments, without the need for expensive facilities. For example, David Werner et al. developed a portable ONT sequencing toolbox targeting 16S rRNA for microbial monitoring at a British wastewater treatment plant and the Akaki River in Ethiopia.[194] This onsite sequencing process can be completed within 1 day, with data analysis available in 24−72 h, demonstrating MinION's potential for rapid pathogen surveillance in outbreak scenarios.

5.3.2. Antibiotic-Resistant Microorganism Analysis. The rapid emergence of antibiotic-resistant bacteria (ARB) poses a significant threat to global public health, as it contributes to the dissemination of ARGs through water, soil and air ecosystems.[195−197] Nanopore sequencing has emerged as a powerful tool for analyzing ARB, offering real-time, long-read sequencing that can identify ARGs and their mobile genetic elements (MGE), such as transposons, plasmids and integrons.[198] Nanopore-based metagenomics has been successfully applied to track the spread of ARGs in environmental sources, such as wastewater treatment plants (WWPT)[199] and agricultural runoff,[200] revealing the diversity and abundance of resistance determinants in these reservoirs. Tools such as NanoARG,[201] NanoOK RT[202] and ARGPore2[199] have been developed to enable ARB and ARG identification in nanopore-based metagenomic data sets. However, like traditional NGS, nanopore metagenomic sequencing is a nontargeted method, which limits its ability to detect low-abundance or rare ARGs. Emerging targeting methods based on CRISPR-Cas9 (context-seq)[174] or single-cell fusion PCR (epicPCR)[203] offer solutions to these sensitivity challenges. For critical ARGs of public health concern, such as the colistin resistance gene, nanopore

https://doi.org/10.1021/jacsau.5c00114
JACS Au 2025, 5, 1570−1590

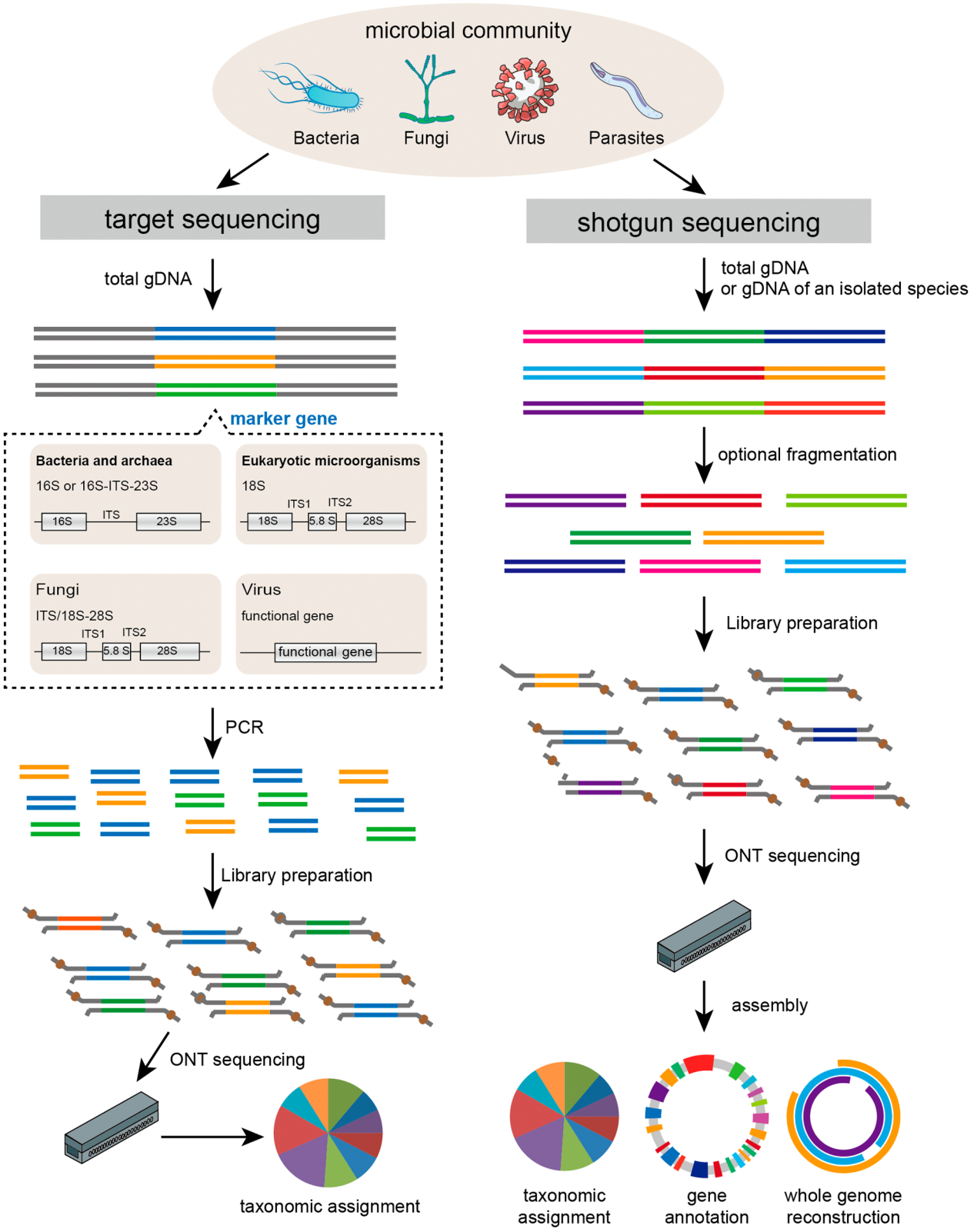

Figure 9. Schematic illustration of nanopore sequencing strategies. Nanopore-based targeted sequencing focuses on specific regions of interest within the genome, offering a cost-effective and faster approach with high accuracy for microorganism taxonomic profiling. Nanopore shotgun sequencing analyses entire genomes or microbial communities, providing a broader view of genetic diversity and functionality but with increased complexity and computational demands.

target sequencing can provide a more comprehensive host profile to complement routine metagenomic screening.

5.3.3. Functional Microorganism Analysis. Functional microorganisms play key roles in shaping and maintaining ecosystem functions through their involvement in critical

https://doi.org/10.1021/jacsau.5c00114
JACS Au 2025, 5, 1570−1590

processes such as biogeochemical cycling, pollutant degradation, and the regulation of ecosystem health.[204] Common functional microorganisms include ammonia-oxidizing bacteria, ammonia-oxidizing archaea, nitrifying bacteria, nitrogen-fixing microorganisms, methanogens, and sulfate-reducing bacteria. Compared with NGS, ONT shotgun sequencing technology enables the acquisition of an almost completely assembled genome, thus helping to discover more unknown microorganisms and new functional genes. In the case of bioremediation, two primary strategies are commonly employed. The first approach focuses on the high-quality whole-genome sequencing of individual microbial species with known functional roles using the combination of the ONT and Illumina NovaSeq platforms.[205] By sequencing the entire genomes of these species, researchers can identify and annotate genes involved in pollutant degradation, such as those involved in metabolic pathways, and encoding enzymes that break down hydrocarbons,[175] heavy metals[178] or dyes.[206] The second approach involves metagenomic sequencing of the entire taxonomic and functional microbiome in activated sludge,[179] wastewater treatment[182] or contaminated environments, such as industrial soil[183] and deep-sea sediments,[207] to more thoroughly understand microbial metabolism and key enzyme-related functional genes, as well as the microbial community structure during bioremediation. Nanopore metagenomic sequencing has revealed microbial communities with the potential to remediate steroids,[208] hexabromocyclododecanes,[209] hydrocarbons,[183] and polychlorinated biphenyls.[184] Although genomics provides valuable information, it does not fully represent the expression, transcription, and corresponding functions of microbial communities. Nanopore-based transcriptomics has also served as a complementary tool to genomics, facilitating a more comprehensive understanding of the functional characteristics of microbial communities.[210]

6. CONCLUSIONS AND OUTLOOK

Nanopore technology is at the forefront of a new era in environmental analysis, offering rapid, sensitive and portable solutions for pollutant monitoring. In this Perspective, we provide a comprehensive review of nanopore technology applications in the environment, highlighting its ability to sense pollutants and to sequence genetic material from microorganisms. Both biological and solid-state nanopores have demonstrated the ability to detect various chemical and biological pollutants. Biological nanopores offer superior signal-to-noise ratios and resolution, whereas solid-state nanopores excel in terms of integration and scalability. In addition to single-molecule sensing, long-read nanopore sequencing is transforming environmental microbiological analyses by providing rapid and detailed insights into microbial diversities, functions, and responses to environmental changes. Portable devices such as Flongle and MinION allow for onsite sequencing, whereas desktop GridION devices enable high-throughput laboratory analyses Despite these advances, real-world nanopore environmental analysis remains challenging.

1. Accurate quantification in environmental matrices. Although the specificity of nanopore sensing can be ensured through customized strategies, in real environmental matrices, the presence of various chemical and biological pollutants will produce nonspecific nanopore events, thus affecting the quantification of the targets. While sample pretreatment methods provide relatively pure samples for quantification, they are time-consuming. Using artificial intelligence algorithms to develop models for matrices effect elimination, target recognition and concentration correlativity building may enable direct quantification in environmental samples.
2. High-throughput detection with nanopore arrays. A single nanopore often requires considerable time to capture sufficient translocation events for reliable detection, especially for low-concentration analytes. Nanopore arrays, by integrating multiple pores into a single device, significantly increase analysis speed and throughput.[211,212] This is particularly beneficial for detecting ultratrace pollutants and enabling rapid on-site or large-scale environmental monitoring. Significant progress has been made in fabricating arrayed biological nanopore platforms (e.g.,16-channel Orbit 16 TC, 512-channel MinION and 14400-channel PromethION) and solid-state nanopore platforms (based on anodic aluminum oxide, silicon, graphene, carbon nanotube and PET).[213,214] Signal crosstalk is a limitation in high-density nanopore arrays, and while precise microelectronic techniques can mitigate this problem, they often come with increased costs.[215] Fluorescence-based nanopore technology, through the use of fluorescently labeled analytes or ionic fluxes, offers a promising alternative by enabling independent detection from multiple nanopores within an array.[216,217]
3. Multitarget analysis with hyphenated technology. Given the increasing diversity of pollutants in environmental samples, combining nanopore technology with other analytical techniques offers great potential for more comprehensive pollutant assessment. In previously study, nanopore technology has been successfully combined with single molecular force spectroscopy,[218] single molecule fluorescence microscopy,[215] Raman spectrum[219] and gel electrophoresis,[220] demonstrating its broad compatibility and versatility. In the future, nanopore technology is expected to be coupled with additional techniques such as chromatography and mass spectrometry. Furthermore, the incorporation of artificial intelligence and machine learning could enable automated analysis and interpretation of multisource data, ultimately facilitating more comprehensive environmental pollutant analysis with broader coverage.
4. Nanopore insights into environmental health. Beyond the detection of environmental pollutants, nanopore technology holds great promise as a powerful tool for studying the molecular toxicology of pollutants. Its ability to provide high-resolution analysis of biomolecular sequences, modifications, structures, and host–guest interactions makes it uniquely suited for understanding the mechanisms by which pollutants affect biological systems.[221,222] Additionally, with significant advancements in protein sequencing and small-molecule sensing, nanopore technology is poised to play a transformative role in advancing environmental multiomics analysis, including genomics, transcriptomics, proteomics, and metabolomics. This integrated approach will provide a comprehensive understanding of the health impacts of pollutants.

Nanopore technology is emerging as a powerful analytical tool in environmental analyses, offering fast monitoring, high

https://doi.org/10.1021/jacsau.5c00114
JACS Au 2025, 5, 1570−1590

resolution, and the ability to analyze a wide range of pollutants and microorganisms simultaneously. Its portability and versatility make it an ideal tool for onsite and comprehensive environmental assessments. We anticipate that nanopore technology will serve as an alternative to traditional analytical techniques and play an increasingly important role in environmental surveillance, ecological governance and sustainable development.

AUTHOR INFORMATION

Corresponding Authors

Shuo Huang − *State Key Laboratory of Analytical Chemistry for Life Sciences, School of Chemistry and Chemical Engineering and Chemistry and Biomedicine Innovation Center (ChemBIC), Nanjing University, Nanjing 210023, China;* orcid.org/0000-0001-6133-7027; Email: shuo.huang@nju.edu.cn

Yuqin Wang − *State Key Laboratory of Pollution Control and Resource Reuse, School of the Environment, Nanjing University, Nanjing 210023, China; Institute for the Environment and Health, Nanjing University Suzhou Campus, Suzhou 215163, China;* orcid.org/0000-0002-9311-241X; Email: yuqinwang@nju.edu.cn

Authors

Xiaofeng Lu − *State Key Laboratory of Pollution Control and Resource Reuse, School of the Environment, Nanjing University, Nanjing 210023, China; Institute for the Environment and Health, Nanjing University Suzhou Campus, Suzhou 215163, China*

Xiaoyu Du − *State Key Laboratory of Pollution Control and Resource Reuse, School of the Environment, Nanjing University, Nanjing 210023, China; Institute for the Environment and Health, Nanjing University Suzhou Campus, Suzhou 215163, China;* orcid.org/0000-0002-4553-8205

Dong Zhong − *State Key Laboratory of Pollution Control and Resource Reuse, School of the Environment, Nanjing University, Nanjing 210023, China; Institute for the Environment and Health, Nanjing University Suzhou Campus, Suzhou 215163, China*

Renjie Li − *State Key Laboratory of Pollution Control and Resource Reuse, School of the Environment, Nanjing University, Nanjing 210023, China; Institute for the Environment and Health, Nanjing University Suzhou Campus, Suzhou 215163, China*

Junjie Cao − *State Key Laboratory of Pollution Control and Resource Reuse, School of the Environment, Nanjing University, Nanjing 210023, China; Institute for the Environment and Health, Nanjing University Suzhou Campus, Suzhou 215163, China*

Complete contact information is available at: https://pubs.acs.org/10.1021/jacsau.5c00114

Author Contributions

[▽]X.L. and X.D. contributed equally.

Funding

This project was funded by the National Key R&D Program of China (Grant No. 2022YFA1304602), the National Natural Science Foundation of China (grant no. 22306089, grant no. 22225405), the Fundamental Research Funds for the Central Universities (grant no. 020514380336), the Programs for High-Level Entrepreneurial and Innovative Talents Introduction of Jiangsu Province (individual and group program), the Excellent Research Program of Nanjing University (grant no. ZYJH004), and the State Key Laboratory of Analytical Chemistry for Life Science (SKLACLS2404).

Notes

The authors declare no competing financial interest.

REFERENCES

(1) Rathi, B. S.; Kumar, P. S.; Vo, D. N. Critical review on hazardous pollutants in water environment: Occurrence, monitoring, fate, removal technologies and risk assessment. *Sci. Total Environ.* **2021**, *797*, No. 149134.

(2) Yu, X.; McPhedran, K. N.; Huang, R. Chlorinated paraffins: A review of sample preparation, instrumental analysis, and occurrence and distribution in food samples. *Environ. Pollut.* **2023**, *318*, No. 120875.

(3) Pan, F.; Yu, Y.; Yu, L.; Lin, H.; Wang, Y.; Zhang, L.; Pan, D.; Zhu, R. Quantitative assessment on soil concentration of heavy metal-contaminated soil with various sample pretreatment techniques and detection methods. *Environ. Monit. Assess.* **2020**, *192* (12), 800.

(4) Cheng, J.; Wang, P.; Su, X.-O. Surface-enhanced raman spectroscopy for polychlorinated biphenyl detection: Recent developments and future prospects. *TrAC, Trends Anal. Chem.* **2020**, *125*, No. 115836.

(5) García-Córcoles, M.; Rodríguez-Gómez, R.; de Alarcón-Gómez, B.; Çipa, M.; Martín-Pozo, L.; Kauffmann, J.-M.; Zafra-Gómez, A. Chromatographic methods for the determination of emerging contaminants in natural water and wastewater samples: A review. *Crit. Rev. Anal. Chem.* **2019**, *49* (2), 160−186.

(6) Hites, R. A. The analysis of organic water pollutants by gas chromatography and gas chromatography-mass spectrometry. *Adv. Chromatogr.* **2024**, 69−112.

(7) Roozbahani, G. M.; Chen, X.; Zhang, Y.; Wang, L.; Guan, X. Nanopore detection of metal ions: Current status and future directions. *Small Methods* **2020**, *4* (10), No. 20200809.

(8) Tanimoto, I. M. F.; Cressiot, B.; Greive, S. J.; Le Pioufle, B.; Bacri, L.; Pelta, J. Focus on using nanopore technology for societal health, environmental, and energy challenges. *Nano Res.* **2022**, *15* (11), 9906−9920.

(9) Ma, W.; Xie, W.; Fang, S.; He, S.; Yin, B.; Wang, Y.; Hou, C.; Huo, D.; Wang, D. Nanopore electrochemical sensors for emerging hazardous pollutants detection. *Electrochim. Acta* **2024**, *475*, No. 143678.

(10) Fan, P.; Cao, Z.; Zhang, S.; Wang, Y.; Xiao, Y.; Jia, W.; Zhang, P.; Huang, S. Nanopore analysis of cis-diols in fruits. *Nat. Commun.* **2024**, *15* (1), 1969.

(11) Jia, W.; Hu, C.; Wang, Y.; Liu, Y.; Wang, L.; Zhang, S.; Zhu, Q.; Gu, Y.; Zhang, P.; Ma, J.; Chen, H. Y.; Huang, S. Identification of single-molecule catecholamine enantiomers using a programmable nanopore. *ACS Nano* **2022**, *16* (4), 6615−6624.

(12) Charles-Achille, S.; Meyer, N.; Abrao-Nemeir, I.; Lepoitevin, M.; Torrent, J.; Janot, J.-M.; Balme, S. Detection and discrimination of nanoparticles using bullet shape nanopores coated with peg. *J. Electroanal. Chem.* **2023**, *939*, No. 117447.

(13) Awasthi, S.; Ying, C.; Li, J.; Mayer, M. Simultaneous determination of the size and shape of single alpha-synuclein oligomers in solution. *ACS Nano* **2023**, *17* (13), 12325−12335.

(14) Arjmandi, N.; Van Roy, W.; Lagae, L.; Borghs, G. Measuring the electric charge and zeta potential of nanometer-sized objects using pyramidal-shaped nanopores. *Anal. Chem.* **2012**, *84* (20), 8490−6.

(15) Galenkamp, N. S.; Biesemans, A.; Maglia, G. Directional conformer exchange in dihydrofolate reductase revealed by single-molecule nanopore recordings. *Nat. Chem.* **2020**, *12* (5), 481−488.

(16) Wei, X.; Wang, Q.; Liu, C. Nanopore sensing of γ-cyclodextrin induced host-guest interaction to reverse the binding of perfluor-

ooctanoic acid to human serum albumin. *Proteomics* **2022**, *22* (5−6), No. 2100058.
(17) Jia, W.; Hu, C.; Wang, Y.; Gu, Y.; Qian, G.; Du, X.; Wang, L.; Liu, Y.; Cao, J.; Zhang, S. Programmable nano-reactors for stochastic sensing. *Nat. Commun.* **2021**, *12* (1), 5811.
(18) Chen, P.; Sun, Z.; Wang, J.; Liu, X.; Bai, Y.; Chen, J.; Liu, A.; Qiao, F.; Chen, Y.; Yuan, C.; Sha, J.; Zhang, J.; Xu, L. Q.; Li, J. Portable nanopore-sequencing technology: Trends in development and applications. *Front. Microbiol.* **2023**, *14*, No. 1043967.
(19) Wang, K.; Zhang, S.; Zhou, X.; Yang, X.; Li, X.; Wang, Y.; Fan, P.; Xiao, Y.; Sun, W.; Zhang, P.; Li, W.; Huang, S. Unambiguous discrimination of all 20 proteinogenic amino acids and their modifications by nanopore. *Nat. Methods* **2024**, *21* (1), 92−101.
(20) Zhang, S.; Cao, Z.; Fan, P.; Sun, W.; Xiao, Y.; Zhang, P.; Wang, Y.; Huang, S. Discrimination of disaccharide isomers of different glycosidic linkages using a modified mspa nanopore. *Angew. Chem., Int. Ed.* **2024**, *63* (8), No. e202316766.
(21) Singh, J.; Yadav, P.; Pal, A. K.; Mishra, V. Water pollutants: Origin and status. *Sensors in water pollutants monitoring: Role of material* **2020**, 5−20.
(22) Liang, L.; Qin, F.; Wang, S.; Wu, J.; Li, R.; Wang, Z.; Ren, M.; Liu, D.; Wang, D.; Astruc, D. Overview of the materials design and sensing strategies of nanopore devices. *Coord. Chem. Rev.* **2023**, *478*, No. 214998.
(23) Dong, L.; Liu, M.; Chen, A.; Wang, Y.; Sun, D. Solubilities of quercetin in three β-cyclodextrin derivative solutions at different temperatures. *J. Mol. Liq.* **2013**, *177*, 204−208.
(24) Ci, Y.; Ma, Y.; Chen, T.; Li, F.; Tang, Y. Facile dissolution of cellulose by superbase-derived ionic liquid using organic solvents as co-solvents at mild temperatures. *Carbohydr. Polym.* **2024**, *330*, No. 121836.
(25) Wang, W.; Ma, X.; Grimes, S.; Cai, H.; Zhang, M. Study on the absorbability, regeneration characteristics and thermal stability of ionic liquids for vocs removal. *Chem. Eng. J.* **2017**, *328*, 353−359.
(26) Han, Y.; Sun, Z.; Sun, Z.; Chen, X.; Zhang, Y.; Sun, Y.; Li, H. Engineering a no-regulated nanofluidic sensor through the cyclization reaction strategy. *Chem.—Eur. J.* **2020**, *26* (49), 11099−11103.
(27) Fujii, S.; Nobukawa, A.; Osaki, T.; Morimoto, Y.; Kamiya, K.; Misawa, N.; Takeuchi, S. Pesticide vapor sensing using an aptamer, nanopore, and agarose gel on a chip. *Lab Chip* **2017**, *17* (14), 2421−2425.
(28) Feng, J.; Liu, K.; Bulushev, R. D.; Khlybov, S.; Dumcenco, D.; Kis, A.; Radenovic, A. Identification of single nucleotides in mos_2 nanopores. *Nat. Nanotechnol* **2015**, *10* (12), 1070−6.
(29) Quan, Q.; Wen, H.; Han, S.; Wang, Z.; Shao, Z.; Chen, M. Fluorous-core nanoparticle-embedded hydrogel synthesized via tandem photo-controlled radical polymerization: Facilitating the separation of perfluorinated alkyl substances from water. *ACS Appl. Mater. Interfaces* **2020**, *12* (21), 24319−24327.
(30) Ighalo, J. O.; Yap, P.-S.; Iwuozor, K. O.; Aniagor, C. O.; Liu, T.; Dulta, K.; Iwuchukwu, F. U.; Rangabhashiyam, S. Adsorption of persistent organic pollutants (pops) from the aqueous environment by nano-adsorbents: A review. *Environ. Res.* **2022**, *212*, No. 113123.
(31) Adeleye, A. S.; Xue, J.; Zhao, Y.; Taylor, A. A.; Zenobio, J. E.; Sun, Y.; Han, Z.; Salawu, O. A.; Zhu, Y. Abundance, fate, and effects of pharmaceuticals and personal care products in aquatic environments. *J. Hazard. Mater. Adv.* **2022**, *424* (Pt B), No. 127284.
(32) Ying, Y.-L.; Hu, Z.-L.; Zhang, S.; Qing, Y.; Fragasso, A.; Maglia, G.; Meller, A.; Bayley, H.; Dekker, C.; Long, Y.-T. Nanopore-based technologies beyond DNA sequencing. *Nat. Nanotechnol.* **2022**, *17* (11), 1136−1146.
(33) Jia, W.; Ouyang, Y.; Zhang, S.; Du, X.; Zhang, P.; Huang, S. Nanopore signatures of nucleoside drugs. *Nano Lett.* **2023**, *23* (20), 9437−9444.
(34) Wang, Y.; Fan, P.; Zhang, S.; Wang, L.; Li, X.; Jia, W.; Liu, Y.; Wang, K.; Du, X.; Zhang, P.; Huang, S. Discrimination of ribonucleoside mono-, di-, and triphosphates using an engineered nanopore. *ACS Nano* **2022**, *16* (12), 21356−21365.
(35) Wang, J.; Prajapati, J. D.; Gao, F.; Ying, Y. L.; Kleinekathofer, U.; Winterhalter, M.; Long, Y. T. Identification of single amino acid chiral and positional isomers using an electrostatically asymmetric nanopore. *J. Am. Chem. Soc.* **2022**, *144* (33), 15072−15078.
(36) Braha, O.; Walker, B.; Cheley, S.; Kasianowicz, J. J.; Song, L.; Gouaux, J. E.; Bayley, H. Designed protein pores as components for biosensors. *Chem. Biol.* **1997**, *4* (7), 497−505.
(37) Cao, J.; Jia, W.; Zhang, J.; Xu, X.; Yan, S.; Wang, Y.; Zhang, P.; Chen, H.-Y.; Huang, S. Giant single molecule chemistry events observed from a tetrachloroaurate(iii) embedded mycobacterium smegmatis porin a nanopore. *Nat. Commun.* **2019**, *10* (1), 5668.
(38) Nestorovich, E. M.; Danelon, C.; Winterhalter, M.; Bezrukov, S. M. Designed to penetrate: Time-resolved interaction of single antibiotic molecules with bacterial pores. *Proc. Natl. Acad. Sci. U.S.A.* **2002**, *99* (15), 9789−9794.
(39) Yao, X.; Song, N.-N.; Wang, J.; Zhao, X.; Cheng, M.-Y.; Zuo, J.; Qiu, K. Influence of electrolyte concentration on single-molecule sensing of perfluorocarboxylic acids. *Front. Chem.* **2021**, *9*, No. 732378.
(40) Wu, Y.; Gooding, J. J. The application of single molecule nanopore sensing for quantitative analysis. *Chem. Soc. Rev.* **2022**, *51* (10), 3862−3885.
(41) Guan, X.; Gu, L. Q.; Cheley, S.; Braha, O.; Bayley, H. Stochastic sensing of tnt with a genetically engineered pore. *ChemBioChem.* **2005**, *6* (10), 1875−81.
(42) Shi, H.-Q.; Ma, Y.; Wang, Y.-H.; Fang, F.; Wu, Z.-Y. Current pulse signature of native kanamycin aptamer and its implication for molecular interactions on a single protein nanopore sensing interface. *Biosens. Bioelectron.* **2022**, *201*, No. 113966.
(43) Su, Z.; Kong, Y.; Li, T.; Zhao, Y.; Zhang, X.; Wu, D.; Wu, Y.; Li, G. An aptamer-triggered hybridization chain reaction strategy for ultra-sensitive biological nanopore detection of aflatoxin b1. *Sens. Actuators, B* **2024**, *407*, No. 135457.
(44) Apetrei, A.; Ciuca, A.; Lee, J.-k.; Seo, C. H.; Park, Y.; Luchian, T. A protein nanopore-based approach for bacteria sensing. *Nanoscale Res. Lett.* **2016**, *11* (1), 501.
(45) Wang, S.; Cao, J.; Jia, W.; Guo, W.; Yan, S.; Wang, Y.; Zhang, P.; Chen, H.-Y.; Huang, S. Single molecule observation of hard−soft-acid−base (hsab) interaction in engineered mycobacterium smegmatis porin a (mspa) nanopores. *Chem. Sci.* **2020**, *11* (3), 879−887.
(46) Song, L.; Hobaugh, M. R.; Shustak, C.; Cheley, S.; Bayley, H.; Gouaux, J. E. Structure of staphylococcal α-hemolysin, a heptameric transmembrane pore. *Science* **1996**, *274* (5294), 1859−1865.
(47) Faller, M.; Niederweis, M.; Schulz, G. E. The structure of a mycobacterial outer-membrane channel. *Science* **2004**, *303* (5661), 1189−1192.
(48) Wang, Y.; Zhang, S.; Jia, W.; Fan, P.; Wang, L.; Li, X.; Chen, J.; Cao, Z.; Du, X.; Liu, Y.; Wang, K.; Hu, C.; Zhang, J.; Hu, J.; Zhang, P.; Chen, H. Y.; Huang, S. Identification of nucleoside monophosphates and their epigenetic modifications using an engineered nanopore. *Nat. Nanotechnol.* **2022**, *17* (9), 976−983.
(49) Wei, X.; Choudhary, A.; Wang, L. Y.; Yang, L.; Uline, M. J.; Tagliazucchi, M.; Wang, Q.; Bedrov, D.; Liu, C. Single-molecule profiling of per- and polyfluoroalkylsubstances by cyclodextrin mediated host-guest interactions within a biological nanopore. *Sci. Adv.* **2024**, *10* (45), 1−16.
(50) Wei, K.; Yao, F.; Kang, X. F. Single-molecule porphyrin-metal ion interaction and sensing application. *Biosens. Bioelectron.* **2018**, *109*, 272−278.
(51) Du, X.; Zhang, S.; Wang, L.; Wang, Y.; Fan, P.; Jia, W.; Zhang, P.; Huang, S. Single-molecule interconversion between chiral configurations of boronate esters observed in a nanoreactor. *ACS Nano* **2023**, *17* (3), 2881−2892.
(52) Wen, S.; Zeng, T.; Liu, L.; Zhao, K.; Zhao, Y. L.; Liu, X. J.; Wu, H. C. Highly sensitive and selective DNA-based detection of mercury(ii) with α-hemolysin nanopore. *J. Am. Chem. Soc.* **2011**, *133* (45), 18312−18317.
(53) Li, T.; Su, Z.; Li, Y.; Xi, L.; Li, G. An aptamer-assisted biological nanopore biosensor for ultra-sensitive detection of ochratoxin a with a

https://doi.org/10.1021/jacsau.5c00114
JACS Au 2025, 5, 1570−1590

portable single-molecule measuring instrument. *Talanta* **2022**, *248*, No. 123619.
(54) Wang, G. H.; Wang, L.; Han, Y. J.; Zhou, S.; Guan, X. Y. Nanopore detection of copper ions using a polyhistidine probe. *Biosens. Bioelectron.* **2014**, *53*, 453−458.
(55) Roozbahani, G. M.; Chen, X.; Zhang, Y.; Juarez, O.; Li, D.; Guan, X. Computation-assisted nanopore detection of thorium ions. *Anal. Chem.* **2018**, *90* (9), 5938−5944.
(56) Roozbahani, G. M.; Chen, X.; Zhang, Y.; Xie, R.; Ma, R.; Li, D.; Li, H.; Guan, X. Peptide-mediated nanopore detection of uranyl ions in aqueous media. *ACS Sens.* **2017**, *2* (5), 703−709.
(57) Stefureac, R. I.; Lee, J. S. Nanopore analysis of the folding of zinc fingers. *Small* **2008**, *4* (10), 1646−1650.
(58) Liu, Y.; Pan, T.; Wang, K.; Wang, Y.; Yan, S.; Wang, L.; Zhang, S.; Du, X.; Jia, W.; Zhang, P. Allosteric switching of calmodulin in a mycobacterium smegmatis porin a (mspa) nanopore-trap. *Angew. Chem., Int. Ed.* **2021**, *60* (44), 23863−23870.
(59) Wang, L.; Yao, F.; Kang, X. F. Nanopore single-molecule analysis of metal ion-chelator chemical reaction. *Anal. Chem.* **2017**, *89* (15), 7958−7965.
(60) Yin, Y.-D.; Yang, L.; Song, X.-T.; Hu, J.; Chen, F.-F.; Xu, M.; Gu, Z.-Y. Determination of acetylamantadine by γ-cyclodextrin-assisted α-hl nanopore for potential cancer prediagnosis. *Anal. Chem.* **2024**, *96* (21), 8325−8331.
(61) Jiang, X.; Zang, M.; Li, F.; Hou, C.; Luo, Q.; Xu, J.; Liu, J. Highly sensitive detection of paraquat with pillar[5]arenes as an aptamer in an α-hemolysin nanopore. *Mater. Chem. Front.* **2021**, *5* (18), 7032−7040.
(62) An, N.; Fleming, A. M.; White, H. S.; Burrows, C. J. Crown ether−electrolyte interactions permit nanopore detection of individual DNA abasic sites in single molecules. *Proc. Natl. Acad. Sci. U. S. A.* **2012**, *109* (29), 11504−11509.
(63) Zhang, Y.; Yi, Y.; Li, Z.; Zhou, K.; Liu, L.; Wu, H.-C. Peptide sequencing based on host−guest interaction-assisted nanopore sensing. *Nat. Methods* **2024**, *21* (1), 102−109.
(64) Reany, O.; Romero-Ruiz, M.; Khurana, R.; Mondal, P.; Keinan, E.; Bayley, H. Stochastic sensing of chloride anions using an α-hemolysin pore with a semiaza-bambusuril adapter. *Angew. Chem.* **2024**, *136* (39), No. e202406719.
(65) Liu, L.; Fang, Z.; Zheng, X.; Xi, D. Nanopore-based strategy for sensing of copper(ii) ion and real-time monitoring of a click reaction. *ACS Sens.* **2019**, *4* (5), 1323−1328.
(66) Liu, G.; Zhang, L.; Dong, D.; Liu, Y.; Li, J. A label-free dnazyme-based nanopore biosensor for highly sensitive and selective lead ion detection. *Anal. Methods* **2016**, *8* (39), 7040−7046.
(67) Braha, O.; Gu, L.-Q.; Zhou, L.; Lu, X.; Cheley, S.; Bayley, H. Simultaneous stochastic sensing of divalent metal ions. *Nat. Biotechnol.* **2000**, *18* (9), 1005−1007.
(68) Cao, J.; Zhang, S.; Zhang, J.; Wang, S.; Jia, W.; Yan, S.; Wang, Y.; Zhang, P.; Chen, H.-Y.; Huang, S. A single-molecule observation of dichloroaurate(i) binding to an engineered mycobacterium smegmatis porin a (mspa) nanopore. *Anal. Chem.* **2021**, *93* (3), 1529−1536.
(69) Yang, C.; Liu, L.; Zeng, T.; Yang, D. W.; Yao, Z. Y.; Zhao, Y. L.; Wu, H. C. Highly sensitive simultaneous detection of lead(ii) and barium(ii) with g-quadruplex DNA in α-hemolysin nanopore. *Anal. Chem.* **2013**, *85* (15), 7302−7307.
(70) Wang, Y.; Luan, B.-Q.; Yang, Z.; Zhang, X.; Ritzo, B.; Gates, K.; Gu, L.-Q. Single molecule investigation of ag^{+} interactions with single cytosine-, methylcytosine-and hydroxymethylcytosine-cytosine mismatches in a nanopore. *Sci. Rep.* **2014**, *4* (1), 5883.
(71) Guo, Y.; Jian, F.; Kang, X. Nanopore sensor for copper ion detection using a polyamine decorated β-cyclodextrin as the recognition element. *RSC Adv.* **2017**, *7* (25), 15315−15320.
(72) Roozbahani, G. M.; Zhang, Y.; Chen, X.; Soflaee, M. H.; Guan, X. Enzymatic reaction-based nanopore detection of zinc ions. *Analyst* **2019**, *144* (24), 7432−7436.
(73) Arora, P.; Zheng, H.; Munusamy, S.; Jahani, R.; Wang, L.; Guan, X. Probe-assisted detection of $fe^{(3+)}$ ions in a multi-functionalized nanopore. *Biosens. Bioelectron.* **2024**, *251*, No. 116125.
(74) Asandei, A.; Apetrei, A.; Luchian, T. Uni-molecular detection and quantification of selected β-lactam antibiotics with a hybrid α-hemolysin protein pore. *J. Mol. Recognit.* **2011**, *24* (2), 199−207.
(75) Yan, S.; Wang, L.; Wang, Y.; Cao, Z.; Zhang, S.; Du, X.; Fan, P.; Zhang, P.; Chen, H. Y.; Huang, S. Non-binary encoded nucleic acid barcodes directly readable by a nanopore. *Angew. Chem., Int. Ed.* **2022**, *61* (20), No. e202116482.
(76) Zhao, C.; Wang, Y.; Chen, C.; Zhu, Y.; Miao, Z.; Mou, X.; Yuan, W.; Zhang, Z.; Li, K.; Chen, M.; Liang, W.; Zhang, M.; Miao, W.; Dong, Y.; Deng, D.; Wu, J.; Ke, B.; Bao, R.; Geng, J. Direct and continuous monitoring of multicomponent antibiotic gentamicin in blood at single-molecule resolution. *ACS Nano* **2024**, *18* (12), 9137−9149.
(77) Júnior, J. J. S.; Soares, T. A.; Pol-Fachin, L.; Machado, D. C.; Rusu, V. H.; Aguiar, J. P.; Rodrigues, C. G. Alpha-hemolysin nanopore allows discrimination of the microcystins variants. *RSC Adv.* **2019**, *9* (26), 14683−14691.
(78) Silva, A.; Silva Junior, J. J. D.; Cavalcanti, M.; Machado, D. C.; Medeiros, P. L.; Rodrigues, C. G. Alphatoxin nanopore detection of aflatoxin, ochratoxin and fumonisin in aqueous solution. *Toxins (Basel)* **2023**, *15* (3), 183.
(79) Zhou, S.; Wang, H.; Chen, X.; Wang, Y.; Zhou, D.; Liang, L.; Wang, L.; Wang, D.; Guan, X. Single-molecule study on interactions between cyclic nonribosomal peptides and protein nanopore. *ACS Appl. Bio Mater.* **2020**, *3* (1), 554−560.
(80) Niu, H.; Zhang, W.; Wei, L.; Liu, M.; Liu, H.; Zhao, C.; Zhang, P.; Liao, Q.; Liu, Y.; Yuan, Q.; Wu, S.; Kang, M.; Geng, J. Rapid nanopore assay for carbapenem-resistant klebsiella pneumoniae. *Front. Microbiol.* **2019**, *10*, 1672.
(81) Oh, S.; Lee, M.-K.; Chi, S.-W. Single-molecule-based detection of conserved influenza a virus rna promoter using a protein nanopore. *ACS Sens.* **2019**, *4* (11), 2849−2853.
(82) Zeng, T.; Li, T.; Li, Y.; Liu, L.; Wang, X.; Liu, Q.; Zhao, Y.; Wu, H.-C. DNA-based detection of mercury(ii) ions through characteristic current signals in nanopores with high sensitivity and selectivity. *Nanoscale* **2014**, *6* (15), 8579−8584.
(83) Asandei, A.; Mereuta, L.; Luchian, T. The kinetics of ampicillin complexation by γ-cyclodextrins. A single molecule approach. *J. Phys. Chem. B* **2011**, *115* (33), 10173−10181.
(84) Wang, Y.; Montana, V.; Grubisic, V.; Stout, R. F., Jr.; Parpura, V.; Gu, L. Q. Nanopore sensing of botulinum toxin type b by discriminating an enzymatically cleaved peptide from a synaptic protein synaptobrevin 2 derivative. *ACS Appl. Mater. Interfaces* **2015**, *7* (1), 184−92.
(85) Wang, L.; Han, Y.; Zhou, S.; Wang, G.; Guan, X. Nanopore biosensor for label-free and real-time detection of anthrax lethal factor. *ACS Appl. Mater. Interfaces* **2014**, *6* (10), 7334−7339.
(86) Li, J.; Stein, D.; McMullan, C.; Branton, D.; Aziz, M. J.; Golovchenko, J. A. Ion-beam sculpting at nanometre length scales. *Nature* **2001**, *412* (6843), 166−169.
(87) Storm, A. J.; Chen, J. H.; Ling, X. S.; Zandbergen, H. W.; Dekker, C. Fabrication of solid-state nanopores with single-nanometre precision. *Nat. Mater.* **2003**, *2* (8), 537−40.
(88) Nam, S.-W.; Rooks, M. J.; Kim, K.-B.; Rossnagel, S. M. Ionic field effect transistors with sub-10 nm multiple nanopores. *Nano Lett.* **2009**, *9* (5), 2044−2048.
(89) Larkin, J.; Henley, R.; Bell, D. C.; Cohen-Karni, T.; Rosenstein, J. K.; Wanunu, M. Slow DNA transport through nanopores in hafnium oxide membranes. *ACS Nano* **2013**, *7* (11), 10121−10128.
(90) Venkatesan, B. M.; Shah, A. B.; Zuo, J. M.; Bashir, R. DNA sensing using nano-crystalline surface enhanced al_2o_3 nanopore sensors. *Adv. Funct Mater.* **2010**, *20* (8), 1266−1275.
(91) Goto, Y.; Yanagi, I.; Matsui, K.; Yokoi, T.; Takeda, K. Integrated solid-state nanopore platform for nanopore fabrication via dielectric breakdown, DNA-speed deceleration and noise reduction. *Sci. Rep* **2016**, *6*, No. 31324.

https://doi.org/10.1021/jacsau.5c00114
JACS Au 2025, 5, 1570−1590

(92) Siwy, Z.; Apel, P.; Baur, D.; Dobrev, D. D.; Korchev, Y. E.; Neumann, R.; Spohr, R.; Trautmann, C.; Voss, K.-O. Preparation of synthetic nanopores with transport properties analogous to biological channels. *Surf. Sci.* **2003**, *532*−*535*, 1061−1066.
(93) Li, W.; Bell, N. A. W.; Hernandez-Ainsa, S.; Thacker, V. V.; Thackray, A. M.; Bujdoso, R.; Keyser, U. F. Single protein molecule detection by glass nanopores. *ACS Nano* **2013**, *7* (5), 4129−4134.
(94) Liu, H.; He, J.; Tang, J.; Liu, H.; Pang, P.; Cao, D.; Krstic, P.; Joseph, S.; Lindsay, S.; Nuckolls, C. Translocation of single-stranded DNA through single-walled carbon nanotubes. *Science* **2010**, *327* (5961), 64−67.
(95) Garaj, S.; Hubbard, W.; Reina, A.; Kong, J.; Branton, D.; Golovchenko, J. A. Graphene as a subnanometre trans-electrode membrane. *Nature* **2010**, *467* (7312), 190−3.
(96) Liu, S.; Lu, B.; Zhao, Q.; Li, J.; Gao, T.; Chen, Y.; Zhang, Y.; Liu, Z.; Fan, Z.; Yang, F.; You, L.; Yu, D. Boron nitride nanopores: Highly sensitive DNA single-molecule detectors. *Adv. Mater.* **2013**, *25* (33), 4549−54.
(97) Mojtabavi, M.; VahidMohammadi, A.; Liang, W.; Beidaghi, M.; Wanunu, M. Single-molecule sensing using nanopores in two-dimensional transition metal carbide (mxene) membranes. *ACS Nano* **2019**, *13* (3), 3042−3053.
(98) Lee, K.; Park, K. B.; Kim, H. J.; Yu, J. S.; Chae, H.; Kim, H. M.; Kim, K. B. Recent progress in solid-state nanopores. *Adv. Mater.* **2018**, *30* (42), No. e1704680.
(99) Xue, L.; Yamazaki, H.; Ren, R.; Wanunu, M.; Ivanov, A. P.; Edel, J. B. Solid-state nanopore sensors. *Nat. Rev. Mater.* **2020**, *5* (12), 931−951.
(100) Xiong, Y.; Ma, T.; Zhang, H.; Qiu, L.; Chang, S.; Yang, Y.; Liang, F. Gold nanoparticle functionalized nanopipette sensors for electrochemical paraquat detection. *Microchim. Acta* **2022**, *189* (7), 251.
(101) Zhang, Y.; Chen, Y.; Fu, Y.; Ying, C.; Feng, Y.; Huang, Q.; Wang, C.; Pei, D.-S.; Wang, D. Monitoring tetracycline through a solid-state nanopore sensor. *Sci. Rep.* **2016**, *6* (1), 27959.
(102) Li, R.; Sui, X.; Li, C.; Jiang, J.; Zhai, J.; Gao, L. Artificial no and light cooperative nanofluidic diode inspired by stomatal closure of guard cells. *ACS Appl. Mater. Interfaces* **2018**, *10* (4), 3241−3247.
(103) Siwy, Z.; Trofin, L.; Kohli, P.; Baker, L. A.; Trautmann, C.; Martin, C. R. Protein biosensors based on biofunctionalized conical gold nanotubes. *J. Am. Chem. Soc.* **2005**, *127* (14), 5000−5001.
(104) Akhtarian, S.; Miri, S.; Doostmohammadi, A.; Brar, S. K.; Rezai, P. Nanopore sensors for viral particle quantification: Current progress and future prospects. *Bioengineered* **2021**, *12* (2), 9189−9215.
(105) Tsutsui, M.; Yokota, K.; Yoshida, T.; Hotehama, C.; Kowada, H.; Esaki, Y.; Taniguchi, M.; Washio, T.; Kawai, T. Identifying single particles in air using a 3d-integrated solid-state pore. *ACS Sens.* **2019**, *4* (3), 748−755.
(106) Cai, Y.; Zhang, B.; Liang, L.; Wang, S.; Zhang, L.; Wang, L.; Cui, H. L.; Zhou, Y.; Wang, D. A solid-state nanopore-based single-molecule approach for label-free characterization of plant polysaccharides. *Plant Commun.* **2021**, *2* (2), No. 100106.
(107) Tsutsui, M.; Yoshida, T.; Yokota, K.; Yasaki, H.; Yasui, T.; Arima, A.; Tonomura, W.; Nagashima, K.; Yanagida, T.; Kaji, N.; Taniguchi, M.; Washio, T.; Baba, Y.; Kawai, T. Discriminating single-bacterial shape using low-aspect-ratio pores. *Sci. Rep.* **2017**, *7* (1), 17371.
(108) Lan, W. J.; Edwards, M. A.; Luo, L.; Perera, R. T.; Wu, X.; Martin, C. R.; White, H. S. Voltage-rectified current and fluid flow in conical nanopores. *Acc. Chem. Res.* **2016**, *49* (11), 2605−2613.
(109) An, P.; Zhang, Z.; Yang, J.; Wang, T.; Wang, Z.; Sun, C.-L.; Qin, C.; Li, J. Ultrasensitive and label-free detection of copper ions by ghk-modified asymmetric nanochannels. *Anal. Chem.* **2023**, *95* (36), 13456−13462.
(110) Qian, Y.; Zhang, Z.; Tian, W.; Wen, L.; Jiang, L. A pb^{2+} ionic gate with enhanced stability and improved sensitivity based on a 4′-aminobenzo-18-crown-6 modified funnel-shaped nanochannel. *Faraday Discuss.* **2018**, *210*, 101−111.
(111) Wu, R.; Zhu, Z.; Xu, X.; Yu, C.; Li, B. An investigation of solid-state nanopores on label-free metal-ion signalling via the transition of rna-cleavage dnazyme and the hybridization chain reaction. *Nanoscale* **2019**, *11* (21), 10339−10347.
(112) Zhai, Q.; Zhang, S.; Jiang, H.; Wei, Q.; Wang, E.; Wang, J. Biomimetic nanopore for sensitive and selective detection of hg(ii) in conjunction with single-walled carbon nanotubes. *J. Mater. Chem. B* **2014**, *2* (37), 6371−6377.
(113) Tian, Y.; Zhang, Z.; Wen, L.; Ma, J.; Zhang, Y.; Liu, W.; Zhai, J.; Jiang, L. A biomimetic mercury(ii)-gated single nanochannel. *Chem. Commun.* **2013**, *49* (91), 10679−81.
(114) Wang, H.; Hou, S.; Wang, Q.; Wang, Z.; Fan, X.; Zhai, J. Dual-response for hg^{2+} and ag^{+} ions based on biomimetic funnel-shaped alumina nanochannels. *J. Mater. Chem. B* **2015**, *3* (8), 1699−1705.
(115) Chen, S.; Chen, H.; Zhang, J.; Dong, H.; Zhan, K.; Tang, Y. A glass nanopore ionic sensor for surface charge analysis. *RSC Adv.* **2020**, *10* (36), 21615−21620.
(116) Zhai, Q.; Wang, J.; Jiang, H.; Wei, Q.; Wang, E. Bare conical nanopore embedded in polymer membrane for cr(iii) sensing. *Talanta* **2015**, *140*, 219−225.
(117) Chen, L.; He, H.; Xu, X.; Jin, Y. Single glass nanopore-based regenerable sensing platforms with a non-immobilized polyglutamic acid probe for selective detection of cupric ions. *Anal. Chim. Acta* **2015**, *889*, 98−105.
(118) Sun, Y.; Zhang, F.; Sun, Z.; Song, M.; Tian, D.; Li, H. Zn^{2+} and edta cooperative switchable nanofluidic diode based on asymmetric modification of single nanochannel. *Chem.—Eur. J.* **2016**, *22* (13), 4355−4358.
(119) Jágerszki, G.; Takács, Á.; Bitter, I.; Gyurcsányi, R. E. Solid-state ion channels forpotentiometric sensing. *Angew. Chem., Int. Ed.* **2011**, *50* (7), 1656−1659.
(120) Niu, B.; Xiao, K.; Huang, X.; Zhang, Z.; Kong, X.-Y.; Wang, Z.; Wen, L.; Jiang, L. High-sensitivity detection of iron(iii) by dopamine-modified funnel-shaped nanochannels. *ACS Appl. Mater. Interfaces* **2018**, *10* (26), 22632−22639.
(121) Ma, T.; Tan, S.; Yuan, R.; Kang, X.; Guo, P.; Tong, Y.; Zhao, T.; Xiao, Z.; Cao, Z.; Li, L.; Balme, S. Highly sensitive and low-cost detecting and recovering ce^{3+} from ammonia nitrogen wastewater using bio-inspired nanochannel/membrane. *Chem. Eng. J.* **2023**, *475*, No. 146084.
(122) Khalid, W.; Abbasi, M. A.; Ali, M.; Ahmad, J.; Ali, Z.; Atif, M.; Ensinger, W. Selective detection of preferential activity of lanthanum ion at zinc oxide functionalized nanochannel. *Nanotechnology* **2021**, *32* (24), No. 245501.
(123) Ali, M.; Ahmed, I.; Ramirez, P.; Nasir, S.; Cervera, J.; Mafe, S.; Niemeyer, C. M.; Ensinger, W. Cesium-induced ionic conduction through a single nanofluidic pore modified with calixcrown moieties. *Langmuir* **2017**, *33* (36), 9170−9177.
(124) Yang, L.; Qian, Y.; Kong, X.-Y.; Si, M.; Zhao, Y.; Niu, B.; Zhao, X.; Wei, Y.; Jiang, L.; Wen, L. Specific recognition of uranyl ion employing a functionalized nanochannel platform for dealing with radioactive contamination. *ACS Appl. Mater. Interfaces* **2020**, *12* (3), 3854−3861.
(125) Tian, Y.; Hou, X.; Wen, L.; Guo, W.; Song, Y.; Sun, H.; Wang, Y.; Jiang, L.; Zhu, D. A biomimetic zinc activated ion channel. *Chem. Commun.* **2010**, *46* (10), 1682.
(126) Zhan, K.; Li, Z.; Chen, J.; Hou, Y.; Zhang, J.; Sun, R.; Bu, Z.; Wang, L.; Wang, M.; Chen, X.; Hou, X. Tannic acid modified single nanopore with multivalent metal ions recognition and ultra-trace level detection. *Nano Today* **2020**, *33*, No. 100868.
(127) Liu, N.; Hou, R.; Gao, P.; Lou, X.; Xia, F. Sensitive $zn^{(2+)}$ sensor based on biofunctionalized nanopores via combination of dnazyme and DNA supersandwich structures. *Analyst* **2016**, *141* (12), 3626−3629.
(128) Bernhard, M.; Diefenbach, M.; Biesalski, M.; Laube, B. Electrical sensing of phosphonates by functional coupling of phosphonate binding protein phnd to solid-state sanopores. *ACS Sens.* **2020**, *5* (1), 234−241.

https://doi.org/10.1021/jacsau.5c00114
JACS Au 2025, 5, 1570−1590

(129) Liu, Q.; Xiao, K.; Wen, L.; Dong, Y.; Xie, G.; Zhang, Z.; Bo, Z.; Jiang, L. A fluoride-driven ionic gate based on a 4-aminophenylboronic acid-functionalized asymmetric single nanochannel. *ACS Nano* **2014**, *8* (12), 12292−12299.
(130) Nie, G.; Sun, Y.; Zhang, F.; Song, M.; Tian, D.; Jiang, L.; Li, H. Fluoride responsive single nanochannel: Click fabrication and highly selective sensing in aqueous solution. *Chem. Sci.* **2015**, *6* (10), 5859−5865.
(131) Xie, G.; Xiao, K.; Zhang, Z.; Kong, X. Y.; Liu, Q.; Li, P.; Wen, L.; Jiang, L. A bioinspired switchable and tunable carbonate-activated nanofluidic diode based on a single nanochannel. *Angew. Chem., Int. Ed.* **2015**, *54* (46), 13664−13668.
(132) Liu, Q.; Wen, L.; Xiao, K.; Lu, H.; Zhang, Z.; Xie, G.; Kong, X. Y.; Bo, Z.; Jiang, L. A biomimetic voltage-gated chloride nanochannel. *Adv. Mater.* **2016**, *28* (16), 3181−3186.
(133) Han, C.; Su, H.; Sun, Z.; Wen, L.; Tian, D.; Xu, K.; Hu, J.; Wang, A.; Li, H.; Jiang, L. Biomimetic ion nanochannels as a highly selective sequential sensor for zinc ions followed by phosphate anions. *Chem.—Eur. J.* **2013**, *19* (28), 9388−9395.
(134) Xia, Z.; Lin, C.-Y.; Drndić, M. Protein-enabled detection of ibuprofen and sulfamethoxazole using solid-state nanopores. *Proteomics* **2022**, *22* (5−6), No. 2100071.
(135) Xu, Y.; Zhang, M.; Tian, T.; Shang, Y.; Meng, Z.; Jiang, J.; Zhai, J.; Wang, Y. Mimicking how plants control co_2 influx: Co_2 activation of ion current rectification in nanochannels. *NPG Asia Mater.* **2015**, *7* (9), No. e215.
(136) Shang, X.; Xie, G.; Kong, X.-Y.; Zhang, Z.; Zhang, Y.; Tian, W.; Wen, L.; Jiang, L. An artificial co_2-driven ionic gate inspired by olfactory sensory neurons in mosquitoes. *Adv. Mater.* **2017**, *29* (3), No. 1603884.
(137) Wu, K.; Kong, X. Y.; Xiao, K.; Wei, Y.; Zhu, C.; Zhou, R.; Si, M.; Wang, J.; Zhang, Y.; Wen, L. Engineered smart gating nanochannels for high performance in formaldehyde detection and removal. *Adv. Funct. Mater.* **2019**, *29* (14), No. 1807953.
(138) Sun, Y.; Chen, S.; Chen, X.; Xu, Y.; Zhang, S.; Ouyang, Q.; Yang, G.; Li, H. A highly selective and recyclable no-responsive nanochannel based on a spiroring opening−closing reaction strategy. *Nat. Commun.* **2019**, *10* (1), 1323.
(139) Ouyang, Q.; Tu, L.; Zhang, Y.; Chen, H.; Fan, Y.; Tu, Y.; Li, Y.; Sun, Y. Construction of a smart nanofluidic sensor through a redox reaction strategy for high-performance carbon monoxide sensing. *Anal. Chem.* **2020**, *92* (22), 14947−14952.
(140) Ding, S.; Gao, C.; Gu, L.-Q. Capturing single molecules of immunoglobulin and ricin with an aptamer-encoded glass nanopore. *Anal. Chem.* **2009**, *81* (16), 6649−6655.
(141) He, F.; Liang, L.; Zhou, S.; Xie, W.; He, S.; Wang, Y.; Tlili, C.; Tong, S.; Wang, D. Label-free sensitive detection of microcystin-lr via aptamer-conjugated gold nanoparticles based on solid-state nanopores. *Langmuir* **2018**, *34* (49), 14825−14833.
(142) Elaguech, M. A.; Yin, Y.; Wang, Y.; Shao, B.; Tlili, C.; Wang, D. Highly sensitive solid-state nanopore aptasensor based on target-induced strand displacement for okadaic acid detection from shellfish samples. *Sens. Diagn.* **2023**, *2* (6), 1612−1622.
(143) McMullen, A.; de Haan, H. W.; Tang, J. X.; Stein, D. Stiff filamentous virus translocations through solid-state nanopores. *Nat. Commun.* **2014**, *5* (1), 4171.
(144) Wu, H.; Chen, Y.; Zhou, Q.; Wang, R.; Xia, B.; Ma, D.; Luo, K.; Liu, Q. Translocation of rigid rod-shaped virus through various solid-state nanopores. *Anal. Chem.* **2016**, *88* (4), 2502−2510.
(145) Tsutsui, M.; Tanaka, M.; Marui, T.; Yokota, K.; Yoshida, T.; Arima, A.; Tonomura, W.; Taniguchi, M.; Washio, T.; Okochi, M.; Kawai, T. Identification of individual bacterial cells through the intermolecular interactions with peptide-functionalized solid-state pores. *Anal. Chem.* **2018**, *90* (3), 1511−1515.
(146) Arima, A.; Harlisa, I. H.; Yoshida, T.; Tsutsui, M.; Tanaka, M.; Yokota, K.; Tonomura, W.; Yasuda, J.; Taniguchi, M.; Washio, T.; Okochi, M.; Kawai, T. Identifying single viruses using biorecognition solid-state nanopores. *J. Am. Chem. Soc.* **2018**, *140* (48), 16834−16841.
(147) Taniguchi, M.; Minami, S.; Ono, C.; Hamajima, R.; Morimura, A.; Hamaguchi, S.; Akeda, Y.; Kanai, Y.; Kobayashi, T.; Kamitani, W.; Terada, Y.; Suzuki, K.; Hatori, N.; Yamagishi, Y.; Washizu, N.; Takei, H.; Sakamoto, O.; Naono, N.; Tatematsu, K.; Washio, T.; Matsuura, Y.; Tomono, K. Combining machine learning and nanopore construction creates an artificial intelligence nanopore for coronavirus detection. *Nat. Commun.* **2021**, *12* (1), 3726.
(148) Niedzwiecki, D. J.; Chou, Y.-C.; Xia, Z.; Thei, F.; Drndić, M. Detection of single analyte and environmental samples with silicon nitride nanopores: Antarctic dirt particulates and DNA in artificial seawater. *Rev. Sci. Instrum.* **2020**, *91* (3), No. 031301.
(149) Zhao, X.-P.; Wang, S.-S.; Younis, M. R.; Xia, X.-H.; Wang, C. Asymmetric nanochannel−ionchannel hybrid for ultrasensitive and label-free detection of copper ions in blood. *Anal. Chem.* **2018**, *90* (1), 896−902.
(150) Arima, A.; Tsutsui, M.; Harlisa, I. H.; Yoshida, T.; Tanaka, M.; Yokota, K.; Tonomura, W.; Taniguchi, M.; Okochi, M.; Washio, T.; Kawai, T. Selective detections of single-viruses using solid-state nanopores. *Sci. Rep.* **2018**, *8* (1), 16305.
(151) AMANN, R.; LUDWIG, W.; SCHLEIFER, K. H. Phylogenetic identification and in situ detection of individual microbial cells without cultivation. *Microbiological Reviews* **1995**, *59* (1), 143−469.
(152) Reuter, J. A.; Spacek, D. V.; Snyder, M. P. High-throughput sequencing technologies. *Mol. Cell* **2015**, *58* (4), 586−597.
(153) Hu, T.; Chitnis, N.; Monos, D.; Dinh, A. Next-generation sequencing technologies: An overview. *Hum. Immunol.* **2021**, *82* (11), 801−811.
(154) Deamer, D.; Akeson, M.; Branton, D. Three decades of nanopore sequencing. *Nat. Biotechnol.* **2016**, *34* (5), 518−524.
(155) Wang, Y.; Zhao, Y.; Bollas, A.; Wang, Y.; Au, K. F. Nanopore sequencing technology, bioinformatics and applications. *Nat. Biotechnol.* **2021**, *39* (11), 1348−1365.
(156) Ni, Y.; Liu, X.; Simeneh, Z. M.; Yang, M.; Li, R. Benchmarking of nanopore r10. 4 and r9. 4.1 flow cells in single-cell whole-genome amplification and whole-genome shotgun sequencing. *Comput. Struct. Biotechnol. J.* **2023**, *21*, 2352−2364.
(157) Payne, A.; Holmes, N.; Rakyan, V.; Loose, M. Bulkvis: A graphical viewer for oxford nanopore bulk fast5 files. *Bioinformatics* **2019**, *35* (13), 2193−2198.
(158) Jenjaroenpun, P.; Wongsurawat, T.; Wadley, T. D.; Wassenaar, T. M.; Liu, J.; Dai, Q.; Wanchai, V.; Akel, N. S.; Jamshidi-Parsian, A.; Franco, A. T.; Boysen, G.; Jennings, M. L.; Ussery, D. W.; He, C.; Nookaew, I. Decoding the epitranscriptional landscape from native rna sequences. *Nucleic Acids Res.* **2021**, *49* (2), No. e7.
(159) Leggett, R. M.; Clark, M. D. A world of opportunities with nanopore sequencing. *J. Exp. Bot.* **2017**, *68* (20), 5419−5429.
(160) Johnson, S. S.; Zaikova, E.; Goerlitz, D. S.; Bai, Y.; Tighe, S. W. Real-time DNA sequencing in the antarctic dry valleys using the oxford nanopore sequencer. *Journal of Biomolecular Techniques* **2017**, *28* (1), 2−7.
(161) Goordial, J.; Altshuler, I.; Hindson, K.; Chan-Yam, K.; Marcolefas, E.; Whyte, L. G. In situ field sequencing and life detection in remote (79 degrees 26′n) canadian high arctic permafrost ice wedge microbial communities. *Front. Microbiol.* **2017**, *8*, 2594.
(162) Gowers, G. F.; Vince, O.; Charles, J. H.; Klarenberg, I.; Ellis, T.; Edwards, A. Entirely off-grid and solar-powered DNA sequencing of microbial communities during an ice cap traverse expedition. *Genes (Basel)* **2019**, *10* (11), 902.
(163) Castro-Wallace, S. L.; Chiu, C. Y.; John, K. K.; Stahl, S. E.; Rubins, K. H.; McIntyre, A. B. R.; Dworkin, J. P.; Lupisella, M. L.; Smith, D. J.; Botkin, D. J.; Stephenson, T. A.; Juul, S.; Turner, D. J.; Izquierdo, F.; Federman, S.; Stryke, D.; Somasekar, S.; Alexander, N.; Yu, G.; Mason, C. E.; Burton, A. S. Nanopore DNA sequencing and genome assembly on the international space station. *Sci. Rep.* **2017**, *7* (1), 18022.
(164) Pinto, Y.; Bhatt, A. S. Sequencing-based analysis of microbiomes. *Nat. Rev. Genet.* **2024**, *25* (12), 829−845.

https://doi.org/10.1021/jacsau.5c00114
JACS Au 2025, 5, 1570−1590

(165) Gołębiewski, M.; Tretyn, A. Generating amplicon reads for microbial community assessment with next-generation sequencing. *J. Appl. Microbiol.* **2020**, *128* (2), 330−354.
(166) Zhang, T.; Li, H.; Ma, S.; Cao, J.; Liao, H.; Huang, Q.; Chen, W. The newest oxford nanopore r10. 4.1 full-length 16s rrna sequencing enables the accurate resolution of species-level microbial community profiling. *Appl. Environ. Microbiol.* **2023**, *89* (10), e00605−23.
(167) Karst, S. M.; Dueholm, M. S.; McIlroy, S. J.; Kirkegaard, R. H.; Nielsen, P. H.; Albertsen, M. Retrieval of a million high-quality, full-length microbial 16s and 18s rrna gene sequences without primer bias. *Nat. Biotechnol.* **2018**, *36* (2), 190−195.
(168) Cuscó, A.; Catozzi, C.; Viñes, J.; Sanchez, A.; Francino, O. Microbiota profiling with long amplicons using nanopore sequencing: Full-length 16s rrna gene and the 16s-its-23s of the rrn operon. *F1000Res.* **2018**, *7*, 1755.
(169) Jain, M.; Abu-Shumays, R.; Olsen, H. E.; Akeson, M. Advances in nanopore direct rna sequencing. *Nat. Methods* **2022**, *19* (10), 1160−1164.
(170) Park, K.; Noh, J.; Kim, K.; Kim, J.; Cho, H.-K.; Kim, S.-G.; Yang, E.; Kim, W.-K.; Song, J.-W. A development of rapid whole-genome sequencing of seoul orthohantavirus using a portable one-step amplicon-based high accuracy nanopore system. *Viruses* **2023**, *15* (7), 1542.
(171) Shaw, A. G.; Majumdar, M.; Troman, C.; O'Toole, Á.; Benny, B.; Abraham, D.; Praharaj, I.; Kang, G.; Sharif, S.; Alam, M. M. Rapid and sensitive direct detection and identification of poliovirus from stool and environmental surveillance samples by use of nanopore sequencing. *J. Clin. Microbiol.* **2020**, *58* (9), 00920−20.
(172) Xu, X.; Deng, Y.; Ding, J.; Tang, Q.; Lin, Y.; Zheng, X.; Zhang, T. High-resolution and real-time wastewater viral surveillance by nanopore sequencing. *Water Res.* **2024**, *256*, No. 121623.
(173) Treagus, S.; Lowther, J.; Longdon, B.; Gaze, W.; Baker-Austin, C.; Ryder, D.; Batista, F. M. Metabarcoding of hepatitis e virus genotype 3 and norovirus gii from wastewater samples in england using nanopore sequencing. *Food Environ. Virol.* **2023**, *15* (4), 292−306.
(174) Fuhrmeister, E. R.; Kim, S.; Mairal, S. A.; McCormack, C.; Chieng, B.; Swarthout, J. M.; Paulos, A. H.; Njenga, S. M.; Pickering, A. J. Context-seq: Crispr-cas9 targeted nanopore sequencing for transmission dynamics of antimicrobial resistance. *bioRxiv* **2024**, 2024.09.12.612745.
(175) Sinha, R. K.; Krishnan, K.; Kurian, P. J. Complete genome sequence and comparative genome analysis of alcanivorax sp. Io_7, a marine alkane-degrading bacterium isolated from hydrothermally-influenced deep seawater of southwest indian ridge. *Genomics* **2021**, *113* (1), 884−891.
(176) Vigil, K.; D'Souza, N.; Bazner, J.; Cedraz, F. M.-A.; Fisch, S.; Rose, J. B.; Aw, T. G. Long-term monitoring of sars-cov-2 variants in wastewater using a coordinated workflow of droplet digital pcr and nanopore sequencing. *Water Res.* **2024**, *254*, No. 121338.
(177) Lee, A. J.; Carson, S.; Reyne, M. I.; Marshall, A.; Moody, D.; Allen, D. M.; Allingham, P.; Levickas, A.; Fitzgerald, A.; Bell, S. H.; Lock, J.; Coey, J. D.; McSparron, C.; Nejad, B. F.; Troendle, E. P.; Simpson, D. A.; Courtney, D. G.; Einarsson, G. G.; McKenna, J. P.; Fairley, D. J.; Curran, T.; McKinley, J. M.; Gilpin, D. F.; Lemon, K.; McGrath, J. W.; Bamford, C. G. G. Wastewater monitoring of human and avian influenza a viruses in northern ireland: A genomic surveillance study. *Lancet Microbe* **2024**, *5* (12), No. 100933.
(178) Sher, S.; Tahir Ishaq, M.; Abbas Bukhari, D.; Rehman, A. Brevibacterium sp. Strain cs2: A potential candidate for arsenic bioremediation from industrial wastewater. *Saudi J. Biol. Sci.* **2023**, *30* (10), No. 103781.
(179) Liu, L.; Wang, Y.; Yang, Y.; Wang, D.; Cheng, S. H.; Zheng, C.; Zhang, T. Charting the complexity of the activated sludge microbiome through a hybrid sequencing strategy. *Microbiome* **2021**, *9* (1), 205.
(180) Gand, M.; Bloemen, B.; Vanneste, K.; Roosens, N. H. C.; De Keersmaecker, S. C. J. Comparison of 6 DNA extraction methods for isolation of high yield of high molecular weight DNA suitable for shotgun metagenomics nanopore sequencing to detect bacteria. *BMC Genomics* **2023**, *24* (1), 438.
(181) Eltokhy, M. A.; Saad, B. T.; Eltayeb, W. N.; Alshahrani, M. Y.; Radwan, S. M. R.; Aboshanab, K. M.; Ashour, M. S. E. Metagenomic nanopore sequencing for exploring the nature of antimicrobial metabolites of bacillus haynesii. *AMB Express* **2024**, *14* (1), 52.
(182) Wang, C.; Wang, Y.; Wang, Y.; Liu, L.; Wang, D.; Ju, F.; Xia, Y.; Zhang, T. Impacts of food waste to sludge ratios on microbial dynamics and functional traits in thermophilic digesters. *Water Res.* **2022**, *219*, No. 118590.
(183) Sandhu, M.; Paul, A. T.; Jha, P. N. Metagenomic analysis for taxonomic and functional potential of polyaromatic hydrocarbons (pahs) and polychlorinated biphenyl (pcb) degrading bacterial communities in steel industrial soil. *PLoS One* **2022**, *17* (4), No. e0266808.
(184) Chakraborty, J.; Rajput, V.; Sapkale, V.; Kamble, S.; Dharne, M. Spatio-temporal resolution of taxonomic and functional microbiome of lonar soda lake of india reveals metabolic potential for bioremediation. *Chemosphere* **2021**, *264*, No. 128574.
(185) Sereika, M.; Kirkegaard, R. H.; Karst, S. M.; Michaelsen, T. Y.; Sorensen, E. A.; Wollenberg, R. D.; Albertsen, M. Oxford nanopore r10.4 long-read sequencing enables the generation of near-finished bacterial genomes from pure cultures and metagenomes without short-read or reference polishing. *Nat. Methods* **2022**, *19* (7), 823−826.
(186) Xia, Y.; Li, X.; Wu, Z.; Nie, C.; Cheng, Z.; Sun, Y.; Liu, L.; Zhang, T. Strategies and tools in illumina and nanopore-integrated metagenomic analysis of microbiome data. *iMeta* **2023**, *2* (1), No. e72.
(187) Singleton, C. M.; Petriglieri, F.; Kristensen, J. M.; Kirkegaard, R. H.; Michaelsen, T. Y.; Andersen, M. H.; Kondrotaite, Z.; Karst, S. M.; Dueholm, M. S.; Nielsen, P. H.; Albertsen, M. Connecting structure to function with the recovery of over 1000 high-quality metagenome-assembled genomes from activated sludge using long-read sequencing. *Nat. Commun.* **2021**, *12* (1), 2009.
(188) Abat, C.; Chaudet, H.; Rolain, J.-M.; Colson, P.; Raoult, D. Traditional and syndromic surveillance of infectious diseases and pathogens. *International Journal of Infectious Diseases* **2016**, *48*, 22−28.
(189) Reska, T.; Pozdniakova, S.; Borràs, S.; Perlas, A.; Sauerborn, E.; Cañas, L.; Schloter, M.; Rodó, X.; Wang, Y.; Winkler, B. Air monitoring by nanopore sequencing. *ISME Commun.* **2024**, *4* (1), No. ycae099.
(190) Nygaard, A. B.; Tunsjo, H. S.; Meisal, R.; Charnock, C. A preliminary study on the potential of nanopore minion and illumina miseq 16s rrna gene sequencing to characterize building-dust microbiomes. *Sci. Rep.* **2020**, *10* (1), 3209.
(191) Urban, L.; Holzer, A.; Baronas, J. J.; Hall, M. B.; Braeuninger-Weimer, P.; Scherm, M. J.; Kunz, D. J.; Perera, S. N.; Martin-Herranz, D. E.; Tipper, E. T.; Salter, S. J.; Stammnitz, M. R. Freshwater monitoring by nanopore sequencing. *eLife* **2021**, *10*, No. e61504.
(192) Quick, J.; Loman, N. J.; Duraffour, S.; Simpson, J. T.; Severi, E.; Cowley, L.; Bore, J. A.; Koundouno, R.; Dudas, G.; Mikhail, A.; Ouédraogo, N.; Afrough, B.; Bah, A.; Baum, J. H. J.; Becker-Ziaja, B.; Boettcher, J. P.; Cabeza-Cabrerizo, M.; Camino-Sánchez, Á.; Carter, L. L.; Doerrbecker, J.; Enkirch, T.; Dorival, I. G.; Hetzelt, N.; Hinzmann, J.; Holm, T.; Kafetzopoulou, L. E.; Koropogui, M.; Kosgey, A.; Kuisma, E.; Logue, C. H.; Mazzarelli, A.; Meisel, S.; Mertens, M.; Michel, J.; Ngabo, D.; Nitzsche, K.; Pallasch, E.; Patrono, L. V.; Portmann, J.; Repits, J. G.; Rickett, N. Y.; Sachse, A.; Singethan, K.; Vitoriano, I.; Yemanaberhan, R. L.; Zekeng, E. G.; Racine, T.; Bello, A.; Sall, A. A.; Faye, O.; Faye, O.; Magassouba, N. F.; Williams, C. V.; Amburgey, V.; Winona, L.; Davis, E.; Gerlach, J.; Washington, F.; Monteil, V.; Jourdain, M.; Bererd, M.; Camara, A.; Somlare, H.; Camara, A.; Gerard, M.; Bado, G.; Baillet, B.; Delaune, D.; Nebie, K. Y.; Diarra, A.; Savane, Y.; Pallawo, R. B.; Gutierrez, G. J.; Milhano, N.; Roger, I.; Williams, C. J.; Yattara, F.; Lewandowski, K.; Taylor, J.; Rachwal, P.; Turner, D. J.; Pollakis, G.; Hiscox, J. A.; Matthews, D. A.; Shea, M. K. O.; Johnston, A. M.; Wilson, D.; Hutley,

https://doi.org/10.1021/jacsau.5c00114
JACS Au 2025, 5, 1570−1590

E.; Smit, E.; Di Caro, A.; Wölfel, R.; Stoecker, K.; Fleischmann, E.; Gabriel, M.; Weller, S. A.; Koivogui, L.; Diallo, B.; Keïta, S.; Rambaut, A.; Formenty, P.; Günther, S.; Carroll, M. W. Real-time, portable genome sequencing for ebola surveillance. *Nature* **2016**, *530* (7589), 228−232.
(193) Oghuan, J.; Chavarria, C.; Vanderwal, S. R.; Gitter, A.; Ojaruega, A. A.; Monserrat, C.; Bauer, C. X.; Brown, E. L.; Cregeen, S. J.; Deegan, J. Wastewater analysis of mpox virus in a city with low prevalence of mpox disease: An environmental surveillance study. *Lancet Regional Health−Americas* **2023**, *28*, No. 100639.
(194) Acharya, K.; Blackburn, A.; Mohammed, J.; Haile, A. T.; Hiruy, A. M.; Werner, D. Metagenomic water quality monitoring with a portable laboratory. *Water Res.* **2020**, *184*, No. 116112.
(195) Wang, J.; Chu, L.; Wojnárovits, L.; Takács, E. Occurrence and fate of antibiotics, antibiotic resistant genes (args) and antibiotic resistant bacteria (arb) in municipal wastewater treatment plant: An overview. *Sci. Total Environ.* **2020**, *744*, No. 140997.
(196) Ondon, B. S.; Li, S.; Zhou, Q.; Li, F. Sources of antibiotic resistant bacteria (arb) and antibiotic resistance genes (args) in the soil: A review of the spreading mechanism and human health risks. *Reviews of Environmental Contamination and Toxicology* **2021**, *256*, 121−153.
(197) Chen, P.; Guo, X.; Li, F. Antibiotic resistance genes in bioaerosols: Emerging, non-ignorable and pernicious pollutants. *J. Cleaner Prod.* **2022**, *348*, No. 131094.
(198) Che, Y.; Xia, Y.; Liu, L.; Li, A.-D.; Yang, Y.; Zhang, T. Mobile antibiotic resistome in wastewater treatment plants revealed by nanopore metagenomic sequencing. *Microbiome* **2019**, *7* (1), 44.
(199) Wu, Z.; Che, Y.; Dang, C.; Zhang, M.; Zhang, X.; Sun, Y.; Li, X.; Zhang, T.; Xia, Y. Nanopore-based long-read metagenomics uncover the resistome intrusion by antibiotic resistant bacteria from treated wastewater in receiving water body. *Water Res.* **2022**, *226*, No. 119282.
(200) Klair, D.; Dobhal, S.; Ahmad, A.; Hassan, Z. U.; Uyeda, J.; Silva, J.; Wang, K.-H.; Kim, S.; Alvarez, A. M.; Arif, M. Exploring taxonomic and functional microbiome of hawaiian stream and spring irrigation water systems using illumina and oxford nanopore sequencing platforms. *Front. Microbiol.* **2023**, *14*, No. 1039292.
(201) Arango-Argoty, G. A.; Dai, D.; Pruden, A.; Vikesland, P.; Heath, L. S.; Zhang, L. Nanoarg: A web service for detecting and contextualizing antimicrobial resistance genes from nanopore-derived metagenomes. *Microbiome* **2019**, *7* (1), 88.
(202) Leggett, R. M.; Alcon-Giner, C.; Heavens, D.; Caim, S.; Brook, T. C.; Kujawska, M.; Martin, S.; Peel, N.; Acford-Palmer, H.; Hoyles, L.; Clarke, P.; Hall, L. J.; Clark, M. D. Rapid minion profiling of preterm microbiota and antimicrobial-resistant pathogens. *Nat. Microbiol.* **2020**, *5* (3), 430−442.
(203) Lou, E. G.; Fu, Y.; Wang, Q.; Treangen, T. J.; Stadler, L. B. Sensitivity and consistency of long-and short-read metagenomics and epicpcr for the detection of antibiotic resistance genes and their bacterial hosts in wastewater. *J. Hazard. Mater.* **2024**, *469*, No. 133939.
(204) Muhammad, S. M.; Saadu, M. Unveiling the roles of microorganisms in promoting environmental sustainability. *Asian Journal of Science, Technology, Engineering, and Art* **2023**, *1* (1), 63−74.
(205) Wick, R. R.; Judd, L. M.; Cerdeira, L. T.; Hawkey, J.; Meric, G.; Vezina, B.; Wyres, K. L.; Holt, K. E. Trycycler: Consensus long-read assemblies for bacterial genomes. *Genome Biol.* **2021**, *22* (1), 266.
(206) Wang, Y.; Cai, X.; Mao, Y. The first complete genome sequence of species shewanella decolorationis, from a bioremediation competent strain ni1−3. *G3-Gens Genomes Genetics* **2021**, *11* (10), No. jkab261.
(207) Marimuthu, J.; Rangamaran, V. R.; Subramanian, S. H. S.; Balachandran, K. R. S.; Kulasekaran, N. T.; Vasudevan, D.; Lee, J.-K.; Ramalingam, K.; Gopal, D. Deep-sea sediment metagenome from bay of bengal reveals distinct microbial diversity and functional significance. *Genomics* **2022**, *114* (6), No. 110524.
(208) Guevara, G.; Espinoza Solorzano, J. S.; Vargas Ramírez, M.; Rusu, A.; Navarro Llorens, J. M. Characterizing a21: Natural cyanobacteria-based consortium with potential for steroid bioremediation in wastewater treatment. *Int. J. Mol. Sci.* **2024**, *25* (23), 13018.
(209) Li, Y. J.; Li, M. H.; Shih, Y. H. Aerobic degradation and the effect of hexabromocyclododecane by soil microbial communities in taiwan. *Environ. Int.* **2020**, *145*, No. 106128.
(210) Tan, L.; Guo, Z.; Shao, Y.; Ye, L.; Wang, M.; Deng, X.; Chen, S.; Li, R. Analysis of bacterial transcriptome and epitranscriptome using nanopore direct rna sequencing. *Nucleic Acids Res.* **2024**, *52* (15), 8746−8762.
(211) Li, Z.-Q.; Huang, L.-Q.; Wang, K.; Xia, X.-H. Developing solid-state single-, arrayed-, and composite-nanopore sensors for biochemical sensing applications. *Acc. Mater. Res.* **2024**, *5* (6), 761−771.
(212) Siwy, Z. S.; Bruening, M. L.; Howorka, S. Nanopores: Synergy from DNA sequencing to industrial filtration - small holes with big impact. *Chem. Soc. Rev.* **2023**, *52* (6), 1983−1994.
(213) Rahman, M.; Sampad, M. J. N.; Hawkins, A.; Schmidt, H. Recent advances in integrated solid-state nanopore sensors. *Lab Chip* **2021**, *21* (16), 3030−3052.
(214) Magierowski, S.; Huang, Y.; Wang, C.; Ghafar-Zadeh, E. Nanopore-cmos interfaces for DNA sequencing. *Biosensors (Basel)* **2016**, *6* (3), 42.
(215) Ivankin, A.; Henley, R. Y.; Larkin, J.; Carson, S.; Toscano, M. L.; Wanunu, M. Label-free optical detection of biomolecular translocation through nanopore arrays. *ACS Nano* **2014**, *8* (10), 10774−10781.
(216) Wang, Y.; Wang, Y.; Du, X.; Yan, S.; Zhang, P.; Chen, H.-Y.; Huang, S. Electrode-free nanopore sensing by diffusioptophysiology. *Sci. Adv.* **2019**, *5* (9), No. eaar3309.
(217) Doan, T. H. P.; Fried, J. P.; Tang, W.; Hagness, D. E.; Wu, Y.; Tilley, R. D.; Gooding, J. J. Optical nanopore blockade sensors for multiplexed detection of proteins. *Nano Lett.* **2025**, *25* (8), 3233−3239.
(218) Tabard-Cossa, V.; Wiggin, M.; Trivedi, D.; Jetha, N. N.; Dwyer, J. R.; Marziali, A. Single-molecule bonds characterized by solid-state nanopore force spectroscopy. *ACS Nano* **2009**, *3* (10), 3009−3014.
(219) Zhou, J.; Lan, Q.; Li, W.; Ji, L.-N.; Wang, K.; Xia, X.-H. Single molecule protein segments sequencing by a plasmonic nanopore. *Nano Lett.* **2023**, *23* (7), 2800−2807.
(220) Chen, K.; Muthukumar, M. Substantial slowing of electrophoretic translocation of DNA through a nanopore using coherent multiple entropic traps. *ACS Nano* **2023**, *17* (10), 9197−9208.
(221) Zhang, Y.; Yi, Y.; Li, Z.; Zhou, K.; Liu, L.; Wu, H. C. Peptide sequencing based on host-guest interaction-assisted nanopore sensing. *Nat. Methods* **2024**, *21* (1), 102−109.
(222) Motone, K.; Kontogiorgos-Heintz, D.; Wee, J.; Kurihara, K.; Yang, S.; Roote, G.; Fox, O. E.; Fang, Y.; Queen, M.; Tolhurst, M.; Cardozo, N.; Jain, M.; Nivala, J. Multi-pass, single-molecule nanopore reading of long protein strands. *Nature* **2024**, *633* (8030), 662−669.

https://doi.org/10.1021/jacsau.5c00114
JACS Au 2025, 5, 1570−1590